CHALMERS
UNIVERSITY OF TECHNOLOGY

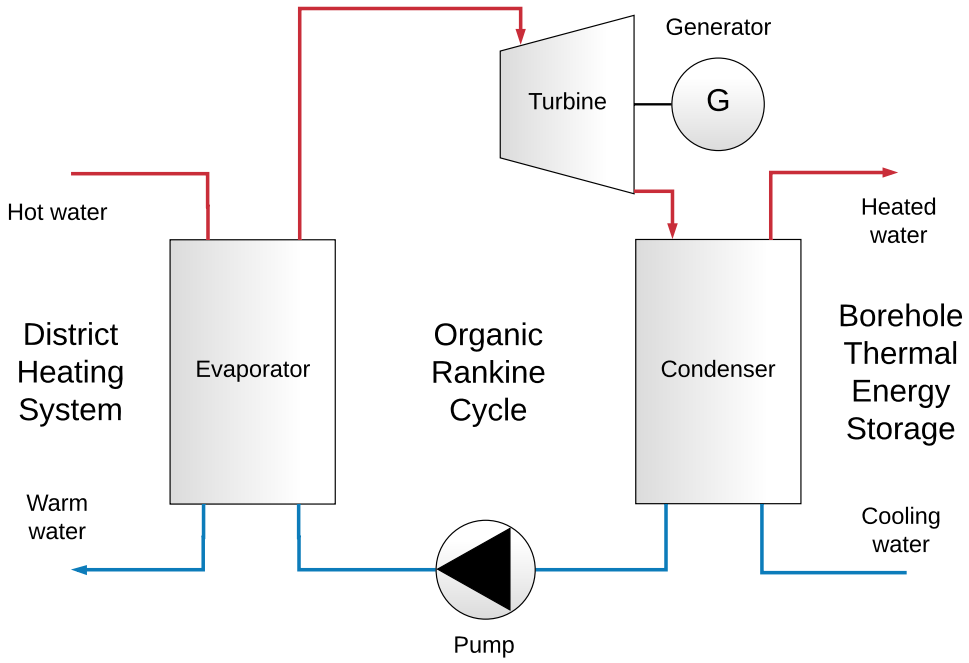

Power production from excess heat in a district heating system

Master's thesis in Sustainable Energy Systems

JONATHAN WINTHER

Department of Architecture and Civil Engineering
CHALMERS UNIVERSITY OF TECHNOLOGY
Gothenburg, Sweden 2018

Master's thesis 2018: ACEX30-18-6

Power production from excess heat in a district heating system

JONATHAN WINTHER

CHALMERS
UNIVERSITY OF TECHNOLOGY

Department of Architecture and Civil Engineering
Division of Building Services Engineering
Chalmers University of Technology
Gothenburg, Sweden 2018

Power production from excess heat in a district heating system
JONATHAN WINTHER

Examiner: Prof. Jan-Olof Dalenbäck, Building Services Engineering
Int. Supervisor: Associate Prof. Saqib Javed, Building Services Engineering
Ext. Supervisor: Lennart Hjalmarsson, Research engineer, Göteborg Energi

Master's Thesis 2018: ACEX30-18-6
Department of Architecture and Civil Engineering
Division of Building Services Engineering
Chalmers University of Technology
SE-412 96 Gothenburg
Telephone +46 31 772 1000

Cover: Circuit of an ORC machine connected with a district heating system and a borehole thermal energy storage.

Typeset in LaTeX
Printed by Chalmers Reproservice
Gothenburg, Sweden 2018

Power production from excess heat in a district heating system
JONATHAN WINTHER
Department of Architecture and Civil Engineering
Chalmers University of Technology

Abstract

Göteborg Energi is contemplating whether excess heat in the district heating (DH) system of Gothenburg can be used to produce electrical power. An ORC solution for electric power production is sought and a handful of options are found. Through an elimination process only one solution remains; an ORC-based heat engine from the company ClimeOn. The heat from the cold side of the ORC machine is stored in a seasonal borehole thermal energy storage (BTES) system. The specifications of the district heating system such as temperatures and flow rates are collected and investigated as well as relevant weather data. A base case is set up as a reference case for comparing the results. A BTES is designed and simulated as well. The placement of the ORC machine within the district heating system of Gothenburg is determined and the power production is also calculated. A sensitivity analysis with different temperatures and flow rates is also carried out and presented. Five other cases are set up from the sensitivity analysis. A life cost analysis is done on all the cases. Three different electricity prices are investigated; 85 SEK/MWh (low), 282.5 SEK/MWh (mean) and 448.4 SEK/MWh (high). The results show that when operating seasonally between May-September the net present value (NPV) is not favourable. However, in Case 5 where an all-year operation is assumed, the NPV is positive if the electricity price is average or above average. A payback period of 10 and 28 years is achieved when considering a high and average electricity price respectively.

Keywords: ORC, District Heating, BTES, Power Production, Waste Heat, ClimeOn, Göteborg Energi.

Acknowledgements

First of all I would like to thank Lennart Hjalmarsson from Göteborg Energi for providing me with this interesting master's thesis as well as supporting me throughout the project by answering all my questions. I would also like to thank Christopher Engman and Johan Larsson for inviting me to an introduction of ClimeOn in Stockholm. The simulation results they provided me was of immense help and really pushed the thesis all the way to the end. Saqib Javed, my supervisor, gave me valuable information regarding borehole thermal energy storage systems and helped me simulate them properly. He also provided me with feedback and pointers on the final report. I am also grateful that the division of building services engineering covered my expenses for travelling to Stockholm. Last, but not least, I would like to thank Jan-Olof Dalenbäck for being my examiner and for taking the time to evaluate this master's thesis.

Jonathan Winther, Gothenburg, 2018

Contents

List of Figures **xi**

List of Tables **xiii**

1 Introduction **1**
1.1 Background . . . 1
1.2 Project aim . . . 2
1.3 Project goals . . . 2
1.4 Scope & limitations . . . 2

2 Theoretical background **3**
2.1 District heating . . . 3
2.1.1 Supply side . . . 3
2.1.2 Consumer side . . . 3
2.1.3 District heating system of Gothenburg . . . 4
2.2 Borehole thermal energy storage . . . 6
2.2.1 Storage type . . . 7
2.2.2 Storage modelling . . . 9
2.2.2.1 BTES simulation softwares . . . 9
2.2.3 Heat pump . . . 10
2.3 Organic rankine cycle . . . 11
2.3.1 Principle . . . 12
2.3.2 Organic fluid . . . 13
2.3.3 Case studies on low-temperature ORC . . . 13
2.3.4 Several commercial companies providing low-temperature ORC-based solutions . . . 15
2.3.4.1 Calnetix . . . 15
2.3.4.2 Climeon . . . 15
2.3.4.3 ElectraTherm . . . 15
2.3.4.4 E-rational . . . 15
2.3.4.5 Orcan Energy AG . . . 16
2.3.4.6 Myriad . . . 16
2.3.4.7 Viking Heat Engines . . . 16
2.4 Electricity price & certificates . . . 16

3 Methods **19**
3.1 Solution . . . 19

3.2 Analysis . . . 20
3.3 BTES design . . . 21
3.4 Base case setup . . . 22
3.5 Calculations . . . 23
3.5.1 Base load . . . 23
3.5.2 Power production . . . 24
3.5.2.1 Sensitivity analysis . . . 25
3.5.3 Additional cases . . . 25
3.5.4 Life cost analysis . . . 26

4 Results **29**
4.1 Chosen ORC-solution . . . 29
4.2 Location . . . 30
4.3 Data simulation . . . 30
4.3.1 BTES . . . 30
4.3.2 Base case . . . 31
4.3.3 Sensitivity analysis . . . 32
4.3.4 Additional cases . . . 34
4.4 Life cost analysis . . . 36

5 Discussion & conclusions **41**

Bibliography **45**

Appendix A District heating system of Gothenburg **I**

Appendix B Prices of electricity certificates **III**

Appendix C Bedrock types in Gothenburg **V**

Appendix D U-tube layout and borehole formation **VII**

Appendix E Climeon technical product sheet **IX**

Appendix F Sensitivity analysis of power production **XI**

List of Figures

2.1 Overview of a district heating system 4
2.2 Correlation between district heating temperature and outdoor temperature (Göteborg Energi, 2016b) 5
2.3 Overview of a BTES system with seasonal storage and a GSHP . . . 7
2.4 The difference between open (a) and closed (b) thermal energy storage systems 8
2.5 Three different types of BHE; Single U-pipe, concentric and double U-pipe 8
2.6 Schematic of a heat pump 11
2.7 Schematic of an ORC with processes 1-4 12

3.1 Base case setup with DH network, ORC machine and BTES system . 24

4.1 Overview of the Climeon ORC machine circuit (ClimeOn, 2017a) . . 30
4.2 Temperature levels for a simulation time period of 25 years from EED4 31
4.3 Power production for different heating and cooling source temperatures at $\dot{q} = 10$ l/s 32
4.4 Power production for different heating and cooling source temperatures at $\dot{q} = 35$ l/s 33
4.5 Power production for different heating and cooling source temperatures at $\dot{q} = 50$ l/s 33
4.6 The net present value over a time period of 30 years considering the low electricity price of 85 SEK/MWh 38
4.7 The net present value over a time period of 30 years considering the mean electricity price of 282.5 SEK/MWh 38
4.8 The net present value over a time period of 30 years considering the high electricity price of 448.4 SEK/MWh 39

A.1 Overview of areas (shown in orange) covered by the district heating system (Göteborg Energi, 2017f) I

B.1 Recent price development of electricity certificates from May-September in 2017 (Energimyndigheten, 2018b) III
B.2 Recent price development of electricity certificates for the year 2017 (Energimyndigheten, 2018b) IV

C.1 Topographical map of the bedrock types in Gothenburg (SGU, Geological Survey of Sweden, 2017) V

D.1 Double u-pipe dimensions of the BTES system VII
D.2 Borehole formation - 7x8 VII

E.1 Parameters for the Climeon Module and Powerblock (ClimeOn, 2017c) IX

List of Tables

2.1 Larger energy producing facilities within the district heating system and their approximate heat production, data from 2016 (Göteborg Energi, 2017d) . . . 5
2.2 Energy prices for district heating in Gothenburg (Göteborg Energi, 2017e) . . . 5
2.3 Properties of different working fluids operating at lower temperatures (Hung et al., 2010; Zhang et al., 2016; DuPont, 2009) . . . 14
2.4 Yearly average electricity price in region SE3 between years 2012-2017 (Nord Pool, 2018) . . . 16

3.1 Eight alternatives for low-temperature power production . . . 20
3.2 Monthly mean outdoor air temperatures for years 2006-2016 (SMHI, 2017) . . . 21
3.3 Calculated monthly mean supply temperatures of the district heating system . . . 21
3.4 Parameters for the bedrock type based in Gothenburg city . . . 22
3.5 Parameters for the borehole, u-pipe and heat carrier fluid . . . 23
3.6 Sensitivity analysis parameters tested for three different water flow rates on both the heating and cooling side . . . 25
3.7 Nominal and real growth rates for the electricity price and electricity certificates . . . 27

4.1 Results for the base case simulation and calculations . . . 31
4.2 Results from Case 1 simulation . . . 34
4.3 Results from Case 2 simulation . . . 34
4.4 Results from Case 3 simulation . . . 35
4.5 Results from Case 4 simulation . . . 35
4.6 Results from Case 5 simulation . . . 36
4.7 Costs related to the Climeon module (ClimeOn, 2017b) . . . 36
4.8 Total net present values for the base case & Cases 1-5 at three different electricity prices . . . 37

F.1 Power production (kW) for different temperatures at a water flow rate of 10 l/s . . . XI
F.2 Power production (kW) for different temperatures at a water flow rate of 35 l/s . . . XI

F.3 Power production (kW) for different temperatures at a water flow rate of 50 l/s XI

Nomenclature

Abbreviations

BHE	Borehole Heat Exchanger
BTES	Borehole Thermal Energy Storage
CHP	Combined Heat-and-Power
DH	District Heating
EED	Earth Energy Designer
GSHP	Ground-Source Heat Pump
HDPE	High-Density Polyethylene
ORC	Organic Rankine Cycle
UTES	Underground Thermal Energy Storage

Symbols & Variables

$\dot{m}$	Mass flow [kg/s]
$\dot{q}$	Flow rate [l/s]
η	Efficiency [-]
ϕ	Specific cost [SEK]
c_p	Specific heat capacity [kJ/kg·K]
COP	Coefficient of performance [-]
E	Energy [Wh]
g	Growth/inflation rate [-]
h	Enthalpy [kJ/kg·K]
I	Investment cost [SEK]
i	Interest rate [-]
NPV	Net present value [SEK]
P	Power [W]
PBP	Payback period [years]
Q	Heat flow [W]
T	Temperature [K]
t	Time [h]
W	Work [W]
X	Unknown constant [-]
Y	Energy price [SEK/MWh]
y	Time period [years]
Z	Annually based cost [SEK/year]

Subscript

$_c$	Cooling
$_h$	Heating
$_m$	Mean

n	Nominal
r	Real
$cert$	Certificate
$cond$	Condenser
el	Electricity
$evap$	Evaporator
gen	Generator
is	Isentropic
max	Maximum

1
Introduction

1.1 Background

The need for heat and electricity has long been known to exist and it is one of the many necessities in modern society. This demand sets high expectations on both reliability and flexibility, which can be provided by energy companies using modern technology. Heat can be distributed and delivered using district heating systems and electricity with the help of the electrical grid system.

In colder regions the usage of district heating is larger than in warmer regions. One particular cold region is Sweden where the concept dates back to the 1940s. Sweden's first district heating system was built in 1948 (Werner, 1989). Today the infrastructure is somewhat different, however, the concept remains the same i.e to provide the surrounding municipality with heat. In Gothenburg, which is a large city in Western Sweden, the district heating system is managed by the energy company Göteborg Energi. The company supplies heat to approximately 90% of all the apartment buildings in the city and surrounding municipalities, as well as to other facilities such as industries and public facilities. The heat consists mainly of waste heat provided by the local combined heat-and-power (CHP) and heating plants (Göteborg Energi, 2017a).

During winter the demand for heat is at its peak, whereas during the summer residual heat is produced due to low heating demand (Göteborg Energi, 2012). One way to utilize this excess heat is to store it seasonally in a low-temperature borehole thermal energy storage (BTES) during periods of low heat demand (Siiskonen, 2015). The stored residual heat can then be extracted when the demand exists.

To further develop the process of storing heat in the BTES an organic rankine cycle (ORC) machine can be connected between the DH system and the BTES, using the excess heat as the driving force for the ORC machine. In this way, electrical power can be produced whilst still providing adequate temperature levels for the district heating system as well as maintaining the low temperature levels used for heat storage in a seasonal BTES.

Göteborg Energi is contemplating whether such a system could be a useful asset to the district heating system of Gothenburg.

1.2 Project aim

The objective of this thesis is to find and evaluate a solution for power production using the district heating system of Gothenburg as the heating source and a BTES as the cooling source. It will be virtually placed in a suitable location within the district heating system and evaluated. Power production and other relevant parameters such as the life cost analysis of the investment are to be calculated and analyzed.

1.3 Project goals

To properly define the project several questions need to be answered. These questions are presented below and constitutes the project goals.

- Where can the solution be placed?
- What are the optimal temperature and mass flow settings for the solution?
- How much electricity can the solution produce?
- How will the energy prices affect the solution?
- Will the solution be profitable?

1.4 Scope & limitations

The thesis will not take into account any new projects affecting either the district heating system or the BTES due to the use of previous statistical data. During calculations parameters such as temperatures and mass flows are considered as constants for simplification purposes, however, different temperatures and mass flows will be tested. Pressure losses in the system are not accounted for due to uncertainty of the components and lack of hands-on testing, especially in the case of the chosen solution.

Any costs or other aspects related to the drilling of a new BTES system or installation of a new heat pump will not be considered and is assumed to already be installed. Selling the heat stored in the BTES or heat costs for the usage of the DH will not be accounted for, as well as heat pump costs. The heat capacity of the district heating system is considered to be unlimited due to the sufficient amount of heat it can provide to the chosen solution. Heat losses within the district heating system will not be relevant as the system is assumed to be ideal.

2
Theoretical background

The thesis uses a variety of terms as it involves concepts including; A district heating system (DH), a low-temperature borehole thermal energy storage (BTES), an organic rankine cycle (ORC) and electricity prices and certificates. These terms will be explained in detail in the following sections.

2.1 District heating

The main purpose of the district heating system is to distribute heat to the surrounding municipality. The heat can come from different sources. Low-grade industrial waste heat and renewable energy sources such as geothermal, solar energy and biomass boilers are some examples (Werner, 2017). The heat travels in isolated ground pipes often using water as the medium. The reason for using water as the circulation medium is the beneficial thermodynamic properties as well as the availability and economical aspect it possesses (Tchanche et al., 2011). A district heating system consists of two parts; the supply side and the consumer side, both connected in a closed-loop system. An overview of the system is presented in Figure 2.1.

2.1.1 Supply side

The supply side is the hot side of the district heating circuit, in which the cold return water from the consumer side is reheated by using a heat exchanger. Heat is usually exchanged with exhaust gas or a steam extraction from e.g. industrial processes or a boiler. In the heat exchanger, the exhaust gas or steam is either cooled down or condensed into liquid due to the sudden temperature drop. The outgoing temperatures of the heat exchanger, supplying the DH heat, are often in the ranges of 60-105°C depending on the desired temperature. The mass flows on the supply side can vary greatly depending on the amount of pumps present (Gadd and Werner, 2014; Lund et al., 2014).

2.1.2 Consumer side

On the consumer side the heat is absorbed by the consumers, or the customers of the energy company. Individual heat exchangers are placed before every facility or building connected to the district heating system to heat up the internal water circuit. The flow rate of the water is easily controlled by adjusting the intake amount using valves. The average return temperature for Swedish district heating systems is 47.2°C (Gadd and Werner, 2014).

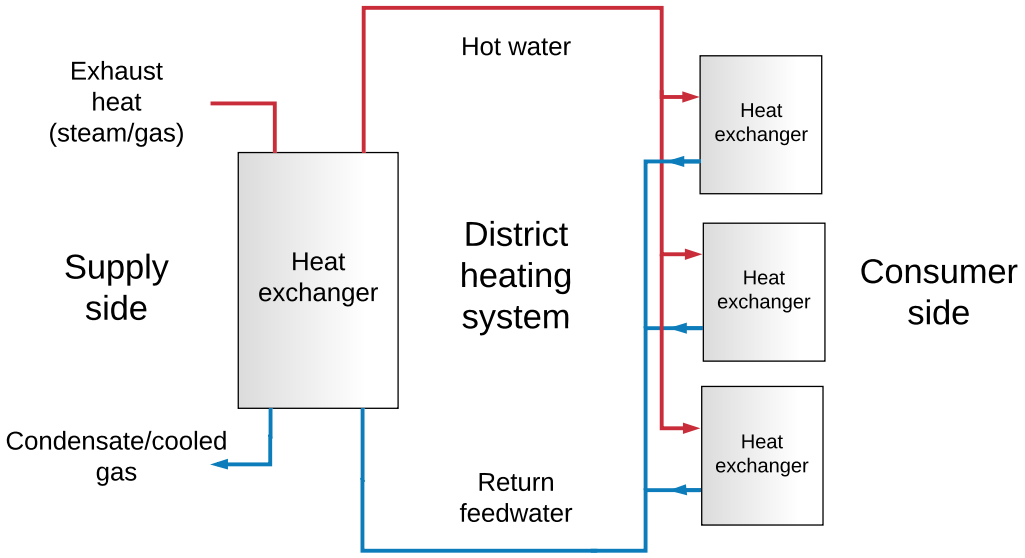

Figure 2.1: Overview of a district heating system

2.1.3 District heating system of Gothenburg

The district heating system of Gothenburg covers a total distance of 1400 km, from Askim to all the way up to Skepplanda, see Appendix A. It has a total production capacity of 1800 MW and a yearly heat production of 3500-5000 GWh, mostly from recycled energy and renewables (Forsgren, 2017). Some part of the heat is provided from the Rya combined heat-and-power (CHP) plant, Rya heat pump plant as well as the heating plant Sävenäs. All three are owned by Göteborg Energi. Waste heat is also provided by the waste CHP plant owned by Renova and the oil refineries owned by St1 and Preem (Göteborg Energi, 2017b). The largest energy producing facilities within the district heating system are summarized in Table 2.1.

The temperature of the hot water supplied from the DH system ranges from 70°C to 105°C depending on the outdoor temperature and the return water temperature is assumed to have an average temperature around 42°C (Göteborg Energi, 2017c). In Figure 2.2, the correlation between district heating and outdoor temperature is presented using two different curves. The red curve shows the curve presented to the customers and has a mean supply temperature of 67°C. However, according to Göteborg Energi the mean supply temperature of 80°C can be used for sizing the ORC solution (Göteborg Energi, 2017d). Hence, the green curve is obtained by approximation.

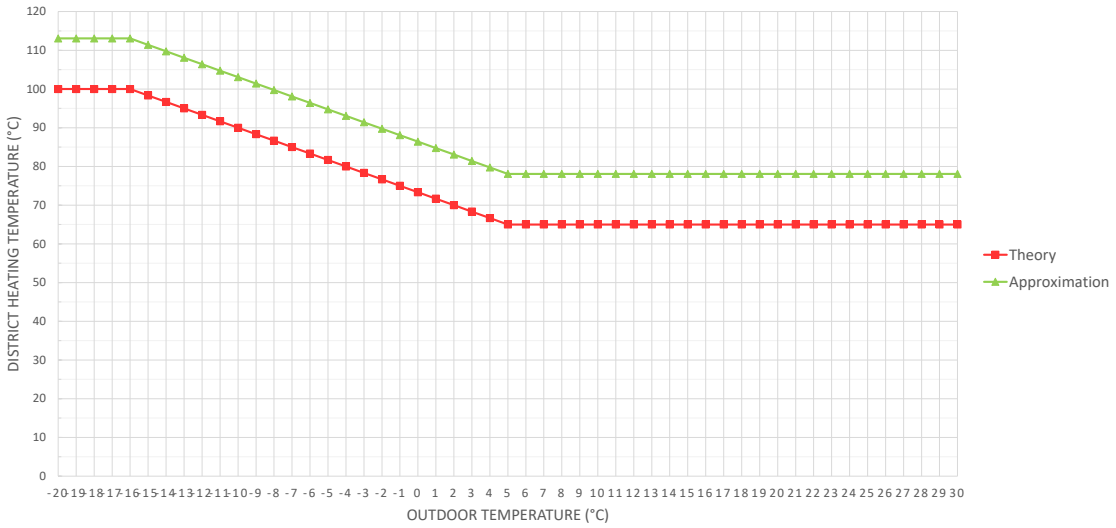

Figure 2.2: Correlation between district heating temperature and outdoor temperature (Göteborg Energi, 2016b)

The energy price of the heat provided by the district heating system is presented in three categories in Table 2.2. The relationship between the three categories winter, autumn/spring and summer relates to the fluctuating demand during the year.

Table 2.1: Larger energy producing facilities within the district heating system and their approximate heat production, data from 2016 (Göteborg Energi, 2017d)

Facility	Approximate heat production (GWh)
Rya heat and power plant	300
Rya heat pump plant	500
Sävenäs plant	400
Oil refineries	1200
Renova heat and power plant	1200

Table 2.2: Energy prices for district heating in Gothenburg (Göteborg Energi, 2017e)

Year	Period	Price (SEK/MWh)
2017	Winter (Jan, Feb, Mars, Dec)	516
	Spring/Autumn (Apr, Oct, Nov)	355
	Summer (May, Jun, Jul, Aug, Sep)	99
2018	Winter (Jan, Feb, Mars, Dec)	519
	Spring/Autumn (Apr, Oct, Nov)	357
	Summer (May, Jun, Jul, Aug, Sep)	99

Mass flows in the system vary depending on the heat demand. Within the district heating system different locations will have different flow rates and this relates to the number of multi-family house buildings present (Göteborg Energi, 2016b). Nevertheless, the district heating system is somewhat flexible in terms of water flow rate and can in most cases provide an adequate flow rate for any situation (Göteborg Energi, 2017d).

2.2 Borehole thermal energy storage

A BTES is a type of underground thermal energy storage (UTES). The general concept of a BTES is to store heat underground where the earth's crust can act as an isolating medium. By drilling deep holes and inserting pipes in the form of heat exchangers, heat can be maintained for a long period of time. Inside the pipes is either water or brine depending on the ground and heat extraction temperatures (Abhat, 1981; Sanner et al., 2003). The boreholes usually have a diameter of around 100-150 mm (Reuss et al., 1997). For underground storage applications seasonal storage is the most common one (Sibbitt et al., 2012), however this choice depends on the area of application.

The depth is an important factor that is strongly considered as different depths may affect the storage temperature. Popiel et al. (2001) presents three different ground depth intervals; Surface zone, Shallow zone and Deep zone with their respective properties.

Surface zone (<1m) - Providing limited isolation abilities this depth is extremely vulnerable to sudden weather and temperature changes.

Shallow zone (1-8m) - This zone provides moderate isolation and only varies seasonally, following the long-term weather changes. The depth for this zone is dependent on the density of the soil and can reach down to 20 metres if the soil proves to be heavy.

Deep zone (>8-20m) - Here temperature changes occur at slower rates. Looking from a seasonal perspective the temperature can be considered constant.

Modern BTES systems always operate within the deep zone due to the fact that it is fairly easy to control the temperature levels and the risk of steep temperature gradients is minimized (Zhai et al., 2011). A common borehole depth is 30-200 meters (Socaciu, 2011). The temperature levels of a BTES system can vary but for a low-temperature system, which is considered in this thesis, the temperature levels are between 0-40°C (Reuss et al., 1997). A simple overview of a BTES system with seasonal storage and a connected ground-source heat pump (GSHP) is presented in Figure 2.3.

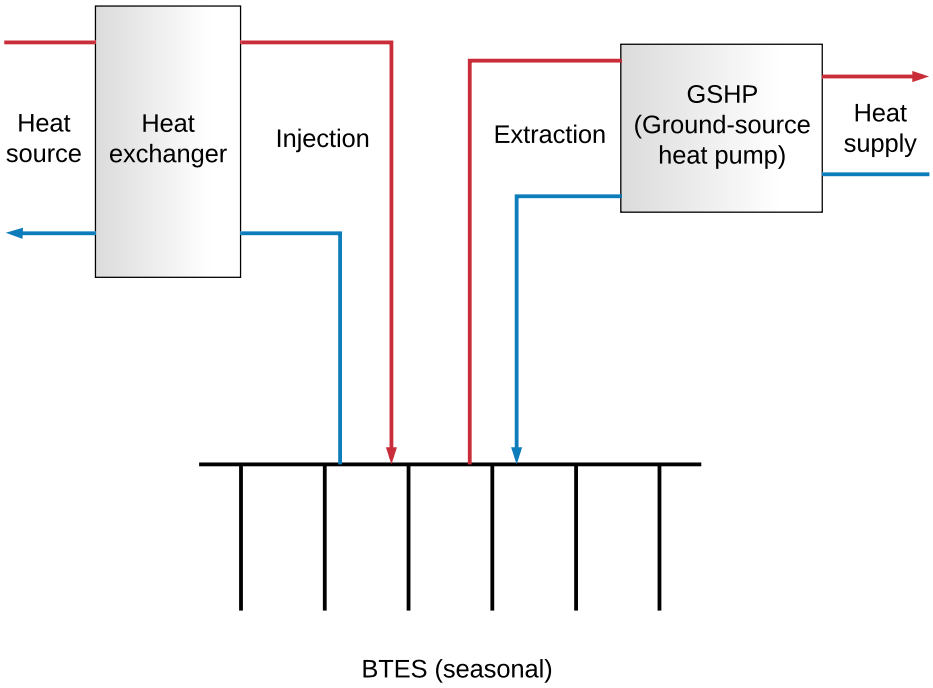

Figure 2.3: Overview of a BTES system with seasonal storage and a GSHP

2.2.1 Storage type

In a BTES, sensible storage is used as it allows for fairly simple designs. The temperature levels are also quite low, which does not indicate a phase-change in commonly used fluids such as water (Socaciu, 2011).

In general there are two types of storage systems; open and closed. A BTES is considered a closed system (ICAX™, 2018). The difference between an open and closed system is that the open system involves having the outlet pipe connected to the deepest end of the borehole and the inlet pipe close to the top end. This allows for direct exchange of fluid inside an aquifer. A closed system however does not allow direct contact of the heat transferring fluid to the surrounding ground as it is inserted as a closed loop. One benefit with this method is that it is not as prone to temperature changes by the surrounding groundwater as the open type (Sang, 2010). It also avoids problems regarding changes in water chemistry due to mixing (Nielsen, 2003; Socaciu, 2011). The two types are presented in Figure 2.4.

Inside the system different borehole heat exchanger (BHE) designs can be constructed. Presented in Figure 2.5 are three common types of BHE (Socaciu, 2011). In the figure the red represents the BHE supply pipe, blue represents the BHE return pipe, gray represents the grouting material and black represents the pipe and borehole walls. Depending on the geometry, thermal conductivity and grout type,

different thermal efficiencies can be achieved (Pahud and Matthey, 2001). The material of the pipes also has an effect on the thermal performance (Schmidt and Mangold, 2006). The ambient climate conditions are also to be considered when choosing the heat exchanger type (Florides and Kalogirou, 2007). When operating at deeper levels within a BTES system the concentric, or coaxial, design proves to be better in terms of hydraulic and thermal optimisation (Rybach and Hopkirk, 1995). Double U-tube configurations reduce the borehole thermal resistance by up to 90% in comparison to single U-tube and is therefore more favorable in terms of thermal performance (Zeng et al., 2003). Lastly, the filling material, also known as grouting is a very important consideration as it ensures good thermal contact with the surrounding ground as well as preventing circulation of ground water (Pahud and Matthey, 2001; Reuss et al., 1997).

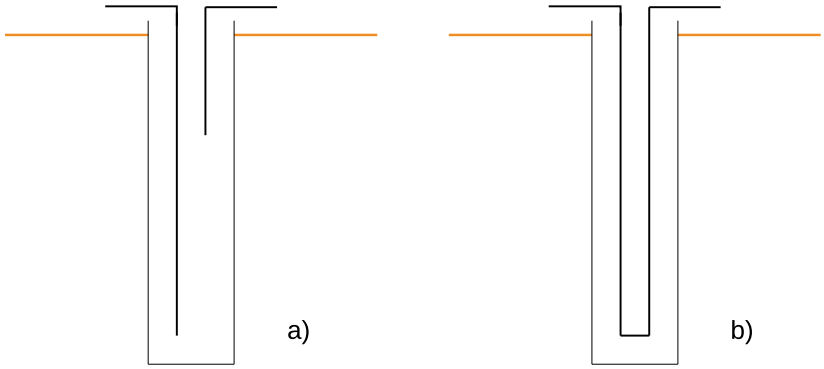

Figure 2.4: The difference between open (a) and closed (b) thermal energy storage systems

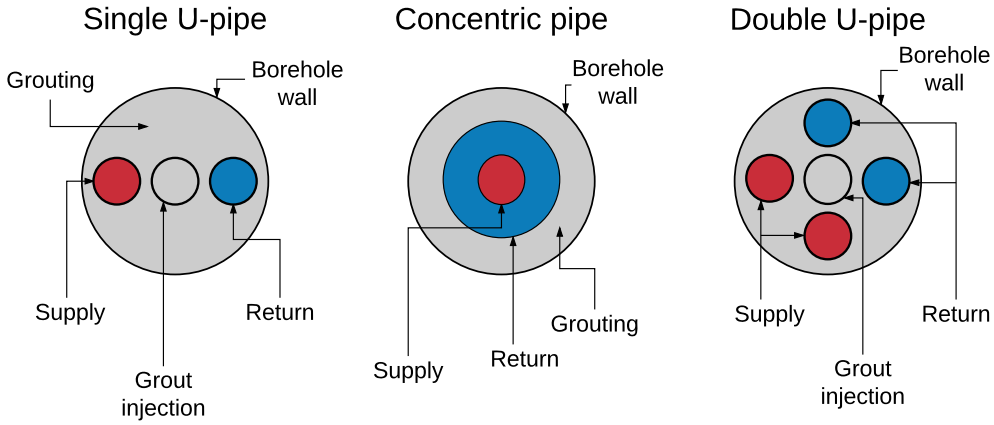

Figure 2.5: Three different types of BHE; Single U-pipe, concentric and double U-pipe

2.2.2 Storage modelling

There are generally three important parameters to take into account when modelling a BTES; the undisturbed ground temperature, ground thermal conductivity and borehole thermal resistance. Both the undisturbed ground temperature and ground thermal conductivity are ground properties fixed for a certain location, which means that the location has to be carefully considered. The thermal resistance is determined by the design parameters of the BTES system.

Undisturbed ground temperature

This parameter is affected by the different ground depth zones explained in Section 2.2. The undisturbed ground temperature increases with increased borehole depth when considering the deep zone. To model this parameter, an average value of the ground temperature is often used (Vieira et al., 2017).

Ground thermal conductivity

The ground thermal conductivity determines the heat transfer rates within the BTES system. This can vary depending on the type of rock that is present at the location. A higher value of the ground thermal conductivity yields higher heat transfer rates (Nordell, 1994).

Borehole thermal resistance

The thermal resistance of a BTES system determines the size of the BHE, the installation costs and the overall performance of the system. It is the thermal resistance between the working fluid and the ground within the system. A low value for the borehole thermal resistance is desirable, as it gives improved heat transfer capacity (Javed and Spitler, 2016; Claesson and Javed, 2018).

2.2.2.1 BTES simulation softwares

In order to simulate a BTES system it must first be modelled properly in a suitable software. There are two different BTES modelling types; duct storage model and superposition borehole model, also known as *g-functions* approach. The duct storage approach has been implemented in the softwares TRNSYS and PILESIM. The g-function approach has been implemented in the simulation softwares GLHEPRO, Polysun and EED. The softwares are briefly described below.

TRNSYS is a software that was first specialized for solar heating simulations. It is very adaptable, as various components can be imported through different libraries. An example of such a library is the TESS package, a library including all the components needed for a simulation of a thermal energy storage system. Locations-based weather data is also available within the software for simulation of different locations (Persson et al., 2016).

PILESIM is an excel-based software that can be used for simulation of BHEs. The simulation software is based on TRNSYS but is more user-friendly. PILESIM can simulate the heating and cooling demands of a building, with the specific heat flows shown in a sankey diagram. However, the software can not take into account smaller BHE systems or uneven borehole formation configurations (Pahud and Fromentin, 1999).

GLHE-PRO is used for simulation of vertical BHEs. The software can perform simulations on a variety of different configurations of a BTES system, approximately 307 different configurations. It can conveniently determine the in- and outgoing temperatures, depth and heat extraction rates of the boreholes in a user-friendly environment (Spitler et al., 2016a).

Polysun is a simulation software adapted for geothermal systems and solar-based applications. To simulate BTES systems, a model called ground source loop must be used. The software can simulate all three BHE types presented in Figure 2.5. Heating and cooling demands for a building can be simulated with different building dimensions and types, along with domestic hot water demand (Persson et al., 2016).

Earth Energy Designer (EED) is a software used for simulation of BTES systems. The main focus of the software is to simulate the BTES system only and therefore the system boundaries are set accordingly. An optimization tool is available within the software to determine borehole depth based on the desired design parameters and results expected (Persson et al., 2016).

Overall, different parameters and properties related to the BTES design must be set in the software used for simulation. In the list below are a few examples of parameters needed for modelling a commercial BTES (Nordell, 1994).

- Storage volume
- Soil cover
- Type of rock
  - Thermal conductivity
  - Thermal capacity
- Storage land area
- Number of boreholes
- Borehole depth
- Borehole spacing
- Borehole diameter
- Circulation system type
- Injected energy/year
- Extracted energy/year
- Max. supply temperature
- Min. leaving temperature
- Heat pumps

2.2.3 Heat pump

A heat pump is used to elevate an existing temperature using a thermodynamic circuit similar to the one of a heat engine, see Section 2.3. The only difference between them is the use of a compressor instead of a turbine and an expanding valve instead of a pump, shown in Figure 2.6. This difference makes $T_{sink} > T_{source}$ and forces the compressor to increase the pressure and temperature of the working fluid with the help of added electrical energy.

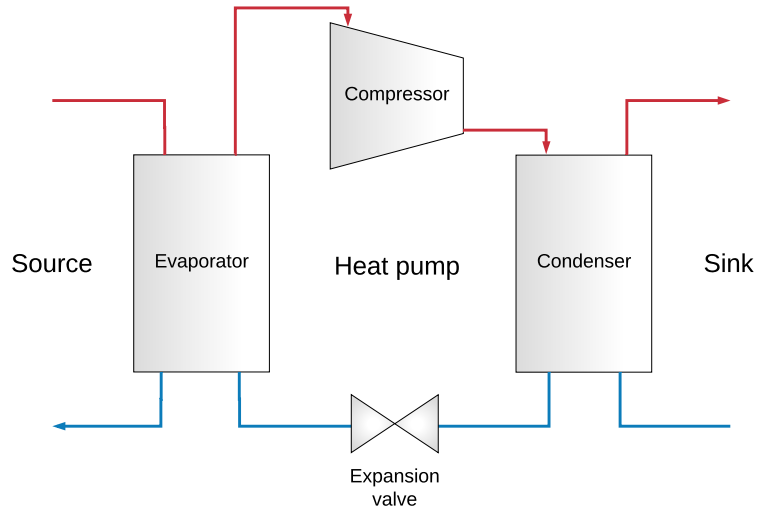

Figure 2.6: Schematic of a heat pump

A heat pump, more specifically a GSHP, is used in a BTES in order to elevate the outgoing temperature when extracting heat from the seasonal storage. The performance of a heat pump is measured as coefficient of performance (COP), shown in Equation 2.1.

$$COP = \frac{Q_{heat}}{W_{el}} = \frac{T_{source}}{T_{sink} - T_{source}} \tag{2.1}$$

Here the outgoing heat is divided by the electrical power consumed to achieve the COP. For this reason the COP is similar to efficiency, but measured for heat pump systems instead. It is always ≥ 1.

2.3 Organic rankine cycle

An ORC is in many ways similar to the traditional rankine cycle with the exception of not using water as the working fluid. Water is inefficient in terms of thermal performance for temperatures under 370°C (Hung et al., 1997; Minea, 2014). An organic fluid is used instead, decreasing the temperature required for the cycle. Other advantages of using an organic fluid includes lower operating pressures and reduced condensation after expansion when using dry fluids (Hung, 2001). The use of single-stage turbines can also decrease the pressure ratio due to the low temperature difference between the evaporator and condenser (Tchanche et al., 2011). Utilizing single-stage ORC systems without reheat or regeneration can also prove to be economically beneficial due to the decreased use of heat exchangers (Erbaş and Biyikoglu, 2013).

2.3.1 Principle

The main purpose of an ORC is to produce useful work from lower temperatures. It does so by taking advantage of a thermodynamic process using two heat exchangers, a pump and a turbine. The circuit requires a heat source and a heat sink in order to operate, with the general principle $T_{source} > T_{sink}$. The maximum theoretical thermal efficiency of an ORC is shown in Equation 2.2. The electrical efficiency of a classic ORC cycle can vary but is around 6.6-7.6% when utilizing a heat source temperature between 85-116°C and a cooling source temperature between 15-30°C (Minea, 2014). In Figure 2.7, the circuit of an ORC is presented.

$$\eta_{max} = \frac{T_{source} - T_{sink}}{T_{source}} \tag{2.2}$$

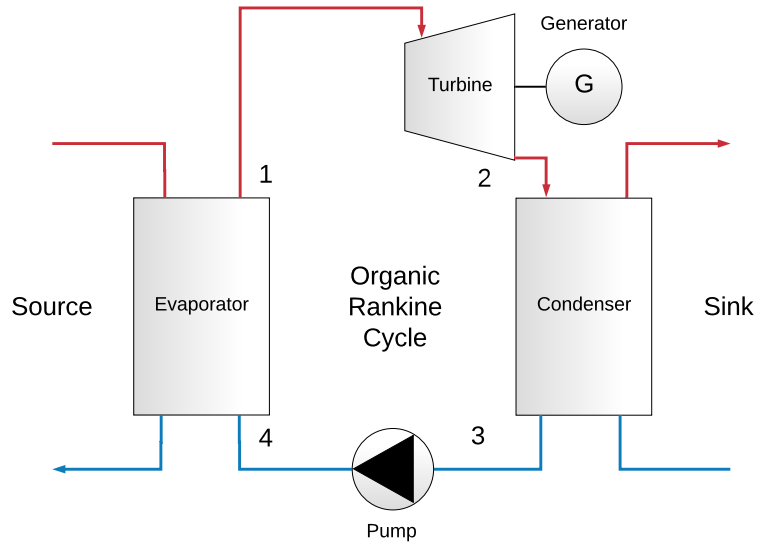

Figure 2.7: Schematic of an ORC with processes 1-4

In process 4-1, a hot and highly pressurized fluid or gas enters the heat exchanger. The heat is transferred to the inner circuit fluid and evaporating it into hot steam, increasing both the temperature and enthalpy greatly. Heat transferred to the working fluid is given by Equation 2.3. Here η_{evap} is the efficiency of the evaporator, $\dot{m}$ is the mass flow rate of the ORC working fluid and h_1 and h_4 are the enthalpies of the outgoing and incoming fluid, respectively, in the evaporator.

$$Q_{evap} = \eta_{evap} \cdot \dot{m} \cdot (h_1 - h_4) \tag{2.3}$$

In process 1-2, the steam is led into a turbine and expanded, thus decreasing pressure, enthalpy and temperature. Momentum from the expansion is then transferred to the connected generator, producing electrical energy. The steam leaving the

turbine can either be wet or dry depending on the pressure drop after expansion. Electricity produced from turbine work is presented in Equation 2.4.

$$P_{el} = \eta_{gen} \cdot \eta_{is} \cdot \dot{m} \cdot (h_1 - h_2) \tag{2.4}$$

In process 2-3, the steam enters the condenser on the heat sink side. The steam is then condensed into liquid by heat rejection in the heat exchanger. This process is both isobaric and isothermal, therefore only the enthalpy is decreased. A common medium for cooling the expanded steam is either water or air. The heat rejected to the cooling medium is shown in Equation 2.5.

$$Q_{cond} = \eta_{cond} \cdot \dot{m} \cdot (h_2 - h_3) \tag{2.5}$$

In process 3-4, the liquid leaving the condenser has a low pressure level, as well as a low enthalpy. To be able to expand in the turbine, the pressure is increased by using a pump or compressor, hence increasing the enthalpy and temperature as well. The pump work is given by Equation 2.6.

$$W_{pump} = \eta_{pump} \cdot \dot{m} \cdot (h_4 - h_3) \tag{2.6}$$

2.3.2 Organic fluid

The organic fluid can be chosen based on the given application. There is no optimal fluid for all cases (Quoilin et al., 2011). However, there are a few organic fluids that are more suitable for temperatures in the lower spectrum, see Table 2.3. These fluids are optimal for ORC-based applications using low-grade waste heat at <100°C and can, for example, be used together with a district heating system. The low boiling point of the working fluids allows for increased fluid pressure as the boiling point increases. Nevertheless, the evaporation temperature should still be under the heat source temperature to allow the fluid to properly evaporate.

2.3.3 Case studies on low-temperature ORC

Previously, there has been a few case studies involving lower ORC temperatures. One particular case is the Paratunka geothermal power plant in eastern Siberia (Moskvicheva and Popov, 1970). It was established in 1967 as a binary power plant and produced both electricity and hot waste water for a nearby village. The plant used the organic working fluid R-12 to power the ORC cycle of the plant and used geothermal wells to extract water at 81°C to evaporate the fluid. A cooling temperature of 14-20°C was utilized and the maximum electrical output was measured to be 340 kW. This is one of the lowest measured heat source temperatures used for power generation reported in literature.

Aneke et al. (2011) presented a computer simulation of the Chena Geothermal Plant in Alaska, performed in the software IPSEpro. This was done to validate the plant's performance at different heat source temperatures. The plant took advantage of the nearby hot springs, delivering a heat source temperature of 73.33°C and a mass flow

rate of 33.39 kg/s. Wet fluid R134a was used as the working fluid in the system and the net power output was measured to 210 kW. The conclusion of the report was that the plant was a feasible solution for low-temperature power generation.

Table 2.3: Properties of different working fluids operating at lower temperatures (Hung et al., 2010; Zhang et al., 2016; DuPont, 2009)

Type	Fluid	$T_{critical}$ (°C)	$P_{critical}$ (MPa)	T_{evap} (°C)	hfg_{atm} (kJ/kg)
Wet fluids	R-11	197.85	4.41	23.05	178.8
	R-12	-161.35	4.125	-29.95	166
	R-134a	101.96	4.0593	-26.07	217.1
	R-152a	116.25	4.45	-25.15	318.4
	R-500	105.45	4.43	-33.65	200.8
	R-502	82.05	4.075	-45.55	172.5
Dry fluids	R-113	214.15	3.41	23.15	182
	R-114	145.85	3.261	3.55	131.8
	R-123	183.75	3.67	27.9	171.5
	R-141b	204.35	4.212	32.05	-
	R-227ea	101.75	2.925	-16.34	131.77
	R-236ea	139.29	3.502	5.8	-
	R-245ca	174.42	3.925	25.13	-
	R-245fa	154.01	3.65	15.14	-
	R-600a	134.66	3.629	-11.8	-

Pikra et al. (2015) presented a geothermal case done in Indonesia. The study involved several different geothermal heat sources ranging from 70-80°C. The goal was to determine the most suitable energy source in terms of location. In the ORC system, R227ea was used as working fluid and 18 different areas were investigated. The study came to the conclusion that only two of the 18 geothermal areas were viable for power production. This was mainly due to the high mass flow rate of the hot water in the springs. An output power of 130.13 kW was ultimately recorded.

Kosmadakis et al. (2016) performed an extensive research on different heat sources and temperatures for an ORC system. The paper presented 16 different cases of ORC power production. The working fluids used were R123, R134a and R245fa with heat source temperatures ranging from 70-100°C. All the cases were simulated using an ORC setup in a laboratory, controlling temperature, mass flows, pressure and heat input accordingly. The rig was coupled with solar PVs and thermal collectors in order to improve the efficiency and the overall results were favorable with respect to the low source temperature.

Kolasiński (2015) published a paper on an ORC study performed in a lab, using an experimental test rig. Heat source temperatures between 40-90°C were tested. The setup used a multivane expander which proved to be very useful when operating at low temperature and pressure levels. A minimum net power output of 123 W and a maximum net power output of 393 W was achieved when using a heat source

temperature of 40°C and 90°C respectively. The paper concluded that a high heat source temperature along with a high expansion ratio was desirable in terms of increasing the net power output.

Borsukiewicz-Gozdur (2013) presented an experimental investigation of an ORC system heat exchanging with a district heating system. The setup used refrigerant R227ea as working fluid and a hot water source temperature of between 66.8-111°C. An overall electrical efficiency of 4.88% was measured for the ORC system.

2.3.4 Several commercial companies providing low-temperature ORC-based solutions

2.3.4.1 Calnetix

Their ORC model Hydrocurrent™ ORC 125EJW utilizes an Integrated Power Module (IPM) with a built-in high-speed turbine expander and a high-efficiency generator coupled in a single casing. The product is specifically made for maritime applications, converting heat from engine jacket water in ships into usable electricity (Calnetix Technologies, 2014). As of 2015 the working fluid R245fa is used in their product (Mitsubishi Heavy Industries Marine Machinery & Engine Co., Ltd., 2015).

2.3.4.2 Climeon

Climeon provides a low temperature solution for power production using a modern ORC setup. Their product come in two different versions; Module and PowerBlock, which are single and serial connected units respectively (ClimeOn, 2017c). The working fluid is currently not disclosed by the company. They are also in possession of several different patented technologies such as their Air Trap Unit (Ahlbom, 2017).

2.3.4.3 ElectraTherm

ElectraTherm have three different models in their product series Power+ Generator™; 4200, 4400 and 6500. The technology uses a twin screw expander together with a generator in order to generate the electricity in the ORC system. The working fluid used is R245fa (ElectraTherm, 2017).

2.3.4.4 E-rational

E-rational provides a compact solution involving a single-screw expander as well as an asynchronous generator. There are three different models, 10FT for indoor applications and 20FT & 40FT for outdoor applications (E-rational, 2017). Refrigerants used as working fluids are either R245fa or SES36 depending on the temperature levels (GB Energy Europe, 2017).

2.3.4.5 Orcan Energy AG

Specialized in energy and fuel savings, Orcan Energy AG supplies a flexible product for low-temperature ORC power production. One of their products is called efficiency Pack or ePack. It is mainly used for marine applications in small freight ships. The working fluid used is not disclosed publically but is known to be a refrigerant of standard sort (Orcan Energy AG, 2017).

2.3.4.6 Myriad

Myriad offers an ORC solution in their Ultra Low Heat (ULH) series, consisting of three different models; ZE-30-ULH, ZE-40-ULH and ZE-50-ULH. The models operate on an unknown mixture of hydro-fluorocarbon based refrigerants (Myriad, 2017).

2.3.4.7 Viking Heat Engines

With the help of an automotive piston-type expander Viking Heat Engines provides a fairly standard ORC solution. Two models are available; CraftEngine CE10 and CraftEngine CE40, which differ in both size and capacity. Working fluid is currently not disclosed (Viking Heat Engines, 2017).

2.4 Electricity price & certificates

The electricity price varies depending on the energy situation with factors such as temperature, weather, day activity, holidays etc. These factors are to a certain extent predictable (Weron, 2014). In Sweden the price is provided by Nord Pool, the leading power market in Europe.

On the market there are different regions depending on the supply and demand of the power market and for Gothenburg the region is called SE3. In Table 2.4, yearly average values (2012-2017) for the electricity price is shown.

Table 2.4: Yearly average electricity price in region SE3 between years 2012-2017 (Nord Pool, 2018)

Year	Electricity price (SEK/MWh)
2017	300.9
2016	277.8
2015	205.9
2014	287.8
2013	340.8
2012	281.9
Average	282.5

Some other interesting numbers during the same set of years and region provided by Nord Pool (2018) are the highest and lowest monthly electricity prices. In February

2012, the highest monthly electricity price was recorded to 448.4 SEK/MWh and, in July 2015, the lowest was recorded to 85.0 SEK/MWh. This clearly shows how the electricity price fluctuates and can affect the solution. Therefore, to simplify calculations, it is recommended to use constant numbers when performing estimations.

To promote the power production from renewable energy sources, an electricity certificate system has been used in Sweden since 2003 (Energimyndigheten, 2018a). The system rewards users of renewables with a certificate that can be sold to electricity market companies or other similar investors for profit. This can be beneficial for an ORC solution as long as the provided heat source is made from renewable energy sources. It is estimated that 12% of the district heating is made from renewable energy sources (Göteborg Energi, 2016a). Figures B.1 and B.2 from Appendix B show example prices for electricity certificates.

3
Methods

The main task of the project was to find a solution for power production within the district heating system. However, various steps were required to reach the intended goal. Firstly a literature study was done to understand the concepts and specifications within the area. Then a handful of solutions were found and an elimination process was used to obtain one final solution. Furthermore, an analysis of the district heating system was done together with collection of relevant weather data. After this a BTES system was designed using the software EED 4 and then a base case of the ORC cycle was set up. This allowed for calculations of the power production as well as doing an accompanying sensitivity analysis. Lastly a life cost analysis was performed.

3.1 Solution

In order to limit the number of solutions, one criterion and one recommendation was set based on the information of the district heating system as well as the BTES. They are presented as follows:

- Minimum temperature requirement for the heat source i.e the hot side of the ORC circuit was set to 80°C. This requirement was based on the mean temperature estimation of the district heating system provided by Göteborg Energi and discussed earlier in Section 2.1.3.

- The cooling temperature from the BTES was designed to be at least 30°C. The BTES operates within this temperature level according to the information given in Section 2.2. However this was not a requirement, but only a recommendation.

After establishing the above mentioned, an online search was conducted to find a suitable solution. Various suitable models were looked at and investigated[1]. Table 3.1 presents these models. For all the models, the criterion for the heating source temperature was expected to be fulfilled.

[1]Data taken from Calnetix Technologies (2014); ClimeOn (2017c); Viking Heat Engines (2017) and ElectraTherm (2017)

Eight different ORC models were found and given as alternatives for the solution of the power production. They all fulfill the requirements for the heating circuit temperatures as they are in the temperature range of the district heating system. However other parameters were not as optimal. The elimination process of the alternatives started with finding a parameter that did not meet the requirement set by both the district heating system and the BTES. If all the requirements were met a second and more strict requirement was set to eliminate further alternatives. The second requirement was to set the minimum heat source temperature to be 70°C. This allows the solution to produce electricity even of temperatures below the mean district heating temperature as well as approaching the minimum DH temperature in Figure 2.2. In the case of not fulfilling the new criteria the solution was eliminated and lastly only one alternative was chosen as the intended solution for the task.

Table 3.1: Eight alternatives for low-temperature power production

	Heating circuit		Cooling circuit		Generator
Product	$\dot{q}$ (l/s)	T (°C)	$\dot{q}$ (l/s)	T (°C)	Power prod. (kW)
Calnetix 125EJW	6.94-61.1	80-95	-	<27	50-125
ClimeOn (Module)	10-50	60-120	10-50	0-35	150
ClimeOn (Powerblock)	70-350	60-120	70-350	0-35	1050
CraftEngine CE40	-	80-200	-	<20	28-30
CraftEngine CE10	-	80-200	-	<20	5-7
Electratherm 4200	3.2-12.6	77-116	13.9	4-65	15 (3.2 l/s, 80°C)
Electratherm 4400	3.2-12.6	77-116	13.9	4-65	15 (3.2 l/s, 80°C)
Electratherm 6500	6.4-22.1	77-122	<22.1	4-65	21 (6.4 l/s, 80°C)

3.2 Analysis

The district heating system of Gothenburg was analyzed based on the information provided in Figure A.1 and Table 2.1 as well as input from Lennart Hjalmarsson (Göteborg Energi, 2017d). As already mentioned in Section 1.4, the heat capacity of the district heating system was considered to be unlimited, hence the placement of the chosen solution was irrelevant in terms of capacity. However, an incentive would be to place it in a location suitable for a BTES system due to the moderate amount of land mass it uses (Nordell, 1994). Another valid reason was to place it close to any of the energy facilities as the water flow rate in the district heating system is higher closer to the providing source. This is due to the branching of the pipes distributing the water (Göteborg Energi, 2017d). Another aspect that was considered as well was a location close to a nearby natural water source. In case the temperature of the BTES would not be sufficient, the option to change cooling source should be available. This can ensure a more reliable, flexible and effective solution.

To know the exact influence of the outdoor temperature on the district heating temperature, statistical weather data was collected. The data represents the monthly mean outdoor air temperatures in Gothenburg during years 2006-2016. It is presented in Table 3.2.

Table 3.2: Monthly mean outdoor air temperatures for years 2006-2016 (SMHI, 2017)

Month	T_m (°C)
January	0.15
February	0.45
March	3.27
April	8.05
May	12.60
June	15.94
July	18.67
August	17.50
September	14.38
October	9.43
November	5.71
December	2.21
Average	**9.03**

Table 3.3: Calculated monthly mean supply temperatures of the district heating system

Month	$T_{supply,m}$ (°C)
January	86.15
February	85.65
March	80.95
April	78.07
May	78.07
June	78.07
July	78.07
August	78.07
September	78.07
October	78.07
November	78.07
December	82.72
Average	**80.00**

The monthly mean outdoor air temperatures were compared to the green curve in the correlation graph of Figure 2.2 to approximate the supply temperatures of the district heating system. Using this approach, a monthly estimate of the supply temperatures could therefore be obtained, as presented in Table 3.3. However due to the limited amount of simulation data of the solution, as well as having close approximation to the monthly average supply temperature, all the months above were given a supply temperature of 80°C when performing calculations.

The monthly mean outdoor air temperatures indicates that the period between May and September is when the temperatures are highest during the year, hence excess heat can be expected to be available during this period due to the lower energy demand. A division was therefore made between October-April and May-September to distinguish between different demand levels. This was also suggested by Göteborg Energi (2017d) as a suitable estimation.

3.3 BTES design

A simple BTES system was designed using the software Earth Energy Designer (EED v4). The parameters set were based on pre-defined settings adjusted for the city of Gothenburg. The model of the BTES was designed in such a way that it uses the ORC circuit as a cooling source based on the calculated heat load levels.

A categorization was made between the different parameters. They are presented below in the following sections.

Ground properties

In Gothenburg the bedrock consists mainly of acidic intrusive rock i.e granite, granodionite or monzonite, as shown in Figure C.1 in Appendix C. Therefore, based on previous experience the following parameters were used for modelling and simulation of the BTES system. These are presented for the ground properties in Table 3.4.

Table 3.4: Parameters for the bedrock type based in Gothenburg city

Parameter	Value	Unit
Bedrock type	Granite	-
Thermal conductivity	3.0	W/m·K
Volumetric heat capacity	2.16	$MJ/m^3 \cdot K$
Ground surface temperature	8	°C
Geothermal heat flux	0.06	W/m^2

BTES properties

The configurations set for these parameters were based on the recommendations and typical values given in Section 2.2, using the double U-tube configuration. The depth, spacing and diameter were all based on typical values for borehole systems (Javed, 2012). The borehole was assumed to be water-filled as typical for BTES systems in Sweden (Javed, 2013). A 7x8 rectangular shape of the borehole pattern was selected as well, presented in Figure D.2 in Appendix D.

For the U-pipe the outer diameter, wall thickness, shank spacing and pipe material were assigned typical values for BTES systems. The pipe material was assumed to be of high-density plastic e.g high-density polyethylene (HDPE). Thermal resistance in the BTES was estimated after the work of Spitler et al. (2016b) and Javed and Spitler (2017). Parameters for both the borehole and U-pipe are presented in Table 3.5. Figure D.1 in Appendix D shows the U-pipe layout.

The selected heat carrier fluid inside the U-pipe was chosen to be a water and ethanol solution. This is due to two main reasons, the first being the availability and second the beneficial thermal properties. It is also estimated that the fluid could reach 0°C and therefore a freezing point below 0°C is desirable.

3.4 Base case setup

In order to prepare for the upcoming calculations, the base case setup was constructed. This case acted as a reference point when performing the power production

calculations and the sensitivity analysis. The circuit of the base case is presented in Figure 3.1.

Table 3.5: Parameters for the borehole, u-pipe and heat carrier fluid

	Parameter	Value	Unit
Borehole	Configuration	7x8	-
	Depth	300	m
	Spacing	7	m
	Diameter	110	mm
	Thermal resistance	0.1	m·K/W
U-pipe	Outer diameter	32	mm
	Wall thickness	3	mm
	Material	HDPE	-
	Thermal conductivity	0.42	W/m·K
	Shank spacing	70	mm
Heat carrier fluid	Water/Ethanol	85/15	%
	Thermal conductivity	0.47	W/(m· K)
	Specific heat capacity	4.373	kJ/(kg· K)
	Density	980	kg/m^3
	Viscosity	0.0042	kg/(m·s)
	Freezing point	-7.2	°C
	Total flow rate	35	l/s

Here, the district heating system act as a heat source for the evaporator, providing the driving force for the ORC cycle. The BTES system on the other hand provides the necessary cooling in the condenser after turbine expansion and consequently reheats the low-temperature water returning to the borehole. With this setup the mean district heating supply temperature of 80°C was used as a reference value together with a condensing temperature of 30°C from the BTES and a total water flow rate of 35 l/s. The same water flow rate is applied on both the heating and cooling sides.

3.5 Calculations

3.5.1 Base load

The base load determines the required heat load levels of the BTES in the simulation software. Monthly values of the base load were calculated based on the two demand levels set earlier between May-September and October-April. It was expected that excess heat from the district heating system is produced between May and September and therefore the solution should primarily be operating during this period. Based on the number of days during different months and the outgoing heat flow of the solution, Equation 3.1 was applied.

$$E_{heat} = \dot{m} \cdot c_p \cdot \Delta T \cdot t \tag{3.1}$$

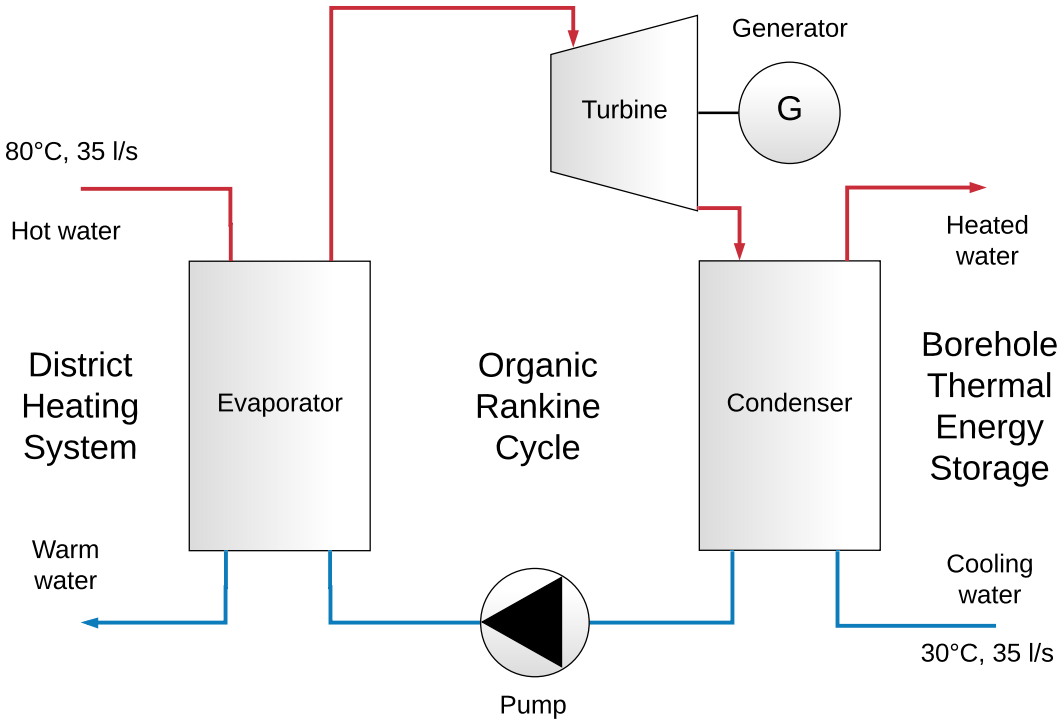

Figure 3.1: Base case setup with DH network, ORC machine and BTES system

Where E_{heat} is the monthly excess heat base load, ΔT represents the temperature difference on the BTES side of the ORC circuit, t is the monthly time measured in hours when excess heat from the district heating system is produced. The base load is given in MWh.

During the time period when the ORC machine is not operating, the excess heat from the BTES will be used to heat nearby buildings, maximizing the usage of the heat storage. Lastly, a simulation period of 25 years was selected in order to properly simulate the BTES for multiple years of operation.

3.5.2 Power production

The calculations for the power production were performed in MATLAB by the suppliers of the ORC solution. Their product is currently in the process of obtaining patents for several of their solutions and a detailed description of the calculations can not be presented. However a simplification was made using the formula for heat transfer presented in Equation 3.2.

$$P_{el} = X \cdot \dot{m} \cdot c_p \cdot \Delta T \tag{3.2}$$

Here X represents a constant based on several different factors affecting the power

production. These factors include the generator and expansion efficiency as well as the influence from the patented technologies. This constant will not be disclosed in this report.

To better compare the power production during operation an additional formula was used to calculate the electrical energy E_{el} in MWh, see Equation 3.3.

$$E_{el} = P_{el} \cdot t \tag{3.3}$$

A few different cases were tested in order to evaluate the power production for different scenarios. These cases represent the main setups that can be used with the solution and indicate how different scenarios affect the power production. The cases all used a water flow of 35 litres per second on both the hot and cold side of the solution to represent an averaged value for the flow of the base cases as well as to simplify the evaluation of the results.

3.5.2.1 Sensitivity analysis

A sensitivity analysis was done to assess the changing seasons and perhaps changes to future temperature levels in the district heating system. The analysis was performed on the heat source temperature, cooling source temperature and water flow rates. In Table 3.6 the different configurations tested are presented with three different water flow rates; 10, 35 and 50 litres per second. The flow rates are assumed to be same for both heating and cooling sides, similar to the base case.

Table 3.6: Sensitivity analysis parameters tested for three different water flow rates on both the heating and cooling side

$\dot{q}$ [l/s]; 10, 35, 50		T_h [°C]			
		70	80	90	100
T_c [°C]	30	x	x	x	x
	25	x	x	x	x
	20	x	x	x	x
	15	x	x	x	x
	10	x	x	x	x

T_h represents the heat source temperatures, T_c the cooling source temperatures and $\dot{q}$ the water flow rates. The x marks the different configurations tested. In total 60 configurations were simulated.

3.5.3 Additional cases

From the sensitivity analysis, a few interesting cases were chosen to be investigated further to determine the best performing configuration. Five additional cases are presented below with their respective parameters.

Case 1

This case involved a decrease of the cooling source temperature from 30°C to 10°C. In this way the influence of a drastic decrease of the cooling temperature was performed. The water flow rate remained the same as in the base case.

Case 2

In Case 2, the heat source temperature was increased from 80°C to 90°C. The cooling source temperature was kept at 30°C and the water flow rate kept at 35 l/s. This case investigates the possibility of an increase in district heating temperature due to, for example, colder climate.

Case 3

Case 3 combined both previous cases resulting in a heat source temperature of 90°C, a cooling source temperature of 10°C and a water flow rate of 35 l/s.

Case 4

This case was designed to test the maximum power production from the ORC machine with the least amount of work input. The heat source temperature was therefore set to 90°C, the cooling source temperature to 10°C and the water flow rate to 50 l/s.

Case 5

In this case it was considered that the ORC solution would be operating all year round. The other parameters were the same as for Case 4, hence providing maximum power production. Therefore the parameters set were T_h = 90°C, T_c = 10°C and $\dot{q}$ = 50 l/s.

3.5.4 Life cost analysis

A life cost analysis was performed considering the investment cost of the solution, the running costs and the revenues from selling produced electricity. There are two interesting parameters to consider when looking to invest in such a product:

- Net present value (NPV)
- Payback period (PBP)

The net present value determines the value of the investment today considering the revenues and costs over a certain time period. The payback period shows the time period at which the investment becomes profitable. This can be determined when the net present value reaches a positive value.

Equation 3.4 below shows the present worth formula for a geometric gradient. Here ϕ_1 is a specific cost at the first year, g the growth rate, i_r the real interest rate,

and y the time period in years. For this work, the nominal interest rate used was 9% and the real interest rate was 7% according to information given by Göteborg Energi (2017d). This gave a general inflation rate of 2%.

$$PV = \phi_1 \left(\frac{1 - (1+g)^y (1+i_r)^{-y}}{i_r - g} \right) \tag{3.4}$$

ϕ_1 is calculated with Equation 3.5.

$$\phi_1 = \phi(1+g) \tag{3.5}$$

The total NPV for the investment was then determined by summarizing the present worth values for the electricity sold and electricity certificates, investment costs and the operating costs. Costs related to the usage of the district heating system was not considered as stated in Section 1.4. The equation for the NPV is shown in Equation 3.6

$$NPV = PV_{CF} - I - PV_Z \tag{3.6}$$

Here, PV_{CF} is the present worth of the electricity and electricity certificates sold, where CF stands for cash flow. The I is the investment cost of the solution and PV_Z is the present worth of an annual cost that was later added as a recommendation for the investment by the ORC company.

In Equation 3.7 the present worth of the cash flow (CF) is calculated with the use of Equation 3.4. Here Y_{el} is the electricity price in SEK/MWh, $Y_{m,cert}$ is the mean electricity certificate price in SEK/MWh when the ORC machine is operating and 0.12 is the share of electricity produced from renewable energy sources (Göteborg Energi, 2016a).

For the base case and Cases 1-4 the electricity certificate prices in Figure B.1 were used and for Case 5 Figure B.2 was used. The growth rate for the electricity price (g_{el}) and the price for electricity certificates (g_{cert}) were calculated from Table 2.4 and acquired from Energimyndigheten (2018b), respectively. The growth rate of the electricity certificate price was based on years 2012-2017, the same as for the electricity price. In Table 3.7, the calculated growth rates, both nominal and real, for the electricity price and electricity certificates are shown.

Table 3.7: Nominal and real growth rates for the electricity price and electricity certificates

Growth rate	Value
$g_{el,n}$	4.0%
$g_{el,r}$	2.0%
$g_{cert,n}$	-0.2%
$g_{cert,r}$	-2.2%

$$PV_{CF} = E_{el} \cdot Y_{el}(1+g_{el})\left(\frac{1-(1+g_{el})^{y}(1+i_r)^{-y}}{i_r - g_{el}}\right) + E_{el} \cdot Y_{cert} \cdot 0.12(1+g_{cert})\left(\frac{1-(1+g_{cert})^{y}(1+i_r)^{-y}}{i_r - g_{cert}}\right) \tag{3.7}$$

Three different electricity prices were investigated; 85.0 SEK/MWh, 282.5 SEK/MWh and 448.4 SEK/MWh to understand the sensitivity of different electricity prices on the NPV. These numbers were previously presented in Section 2.4 and refer to a low, mean and high electricity price respectively.

Equation 3.8 shows the calculation of the present worth for the recommended annual cost added to the investment. Here the general growth rate g was taken to be equal to inflation, i.e the real price growth = 0.

$$PV_Z = Z(1+g)\left(\frac{1-(1+g)^{y}(1+i_r)^{-y}}{i_r - g}\right) \tag{3.8}$$

The payback period (PBP) was determined graphically by calculating the NPV for each year within the time period y until a positive NPV was obtained. For this solution the time period y was set to 30 years according to information given by the ORC company.

4
Results

4.1 Chosen ORC-solution

The chosen solution for the power production was the Climeon module. The chosen solution is an ORC-based heat engine that is able to produce power using DH temperatures down to 60°C. This ensures a viable solution even if the DH supply temperatures decreases in the future. An overview of the module circuit is presented in Figure 4.1. The Climeon module utilizes the so-called C3 technology (ClimeOn, 2017b), involving three key parts for the power generation.

- A partial vacuum that is created within the system to reduce the pressure after the expansion. This helps reduce the construction materials needed, improves efficiency as well as decrease the size of the pumps in the system. The vacuum is created with the Air Trap Unit, a patented technology from Climeon (Ahlbom, 2017).

- The working fluid used is perfectly adapted to the module system and was chosen amongst a myriad of other alternatives. However, it is currently not disclosed.

- Within the system cold working fluid is sprayed in the condenser and onto the warmer working fluid after expansion. This is done to reduce temperature levels quickly, resulting in reduced heat losses. It is done in a closed loop, utilizing a feedback connection between the condenser and cooling part of the circuit.

As introduced in the C3 technology, the product involves a branching of the working fluid after condensation. This is different from the traditional ORC cycle. In this case the working fluid is partially split, and is either recirculated back to the condenser or pressurized by the pump before evaporation. Two pumps are also present in the circuit, one positioned directly before entering the evaporator and one positioned directly after the condensation spraying. The heat exchangers used are two plate heat exchangers, both of which are positioned on the evaporation and condensation sides respectively.

Additional information regarding their product is presented in Figure E.1 in Appendix E.

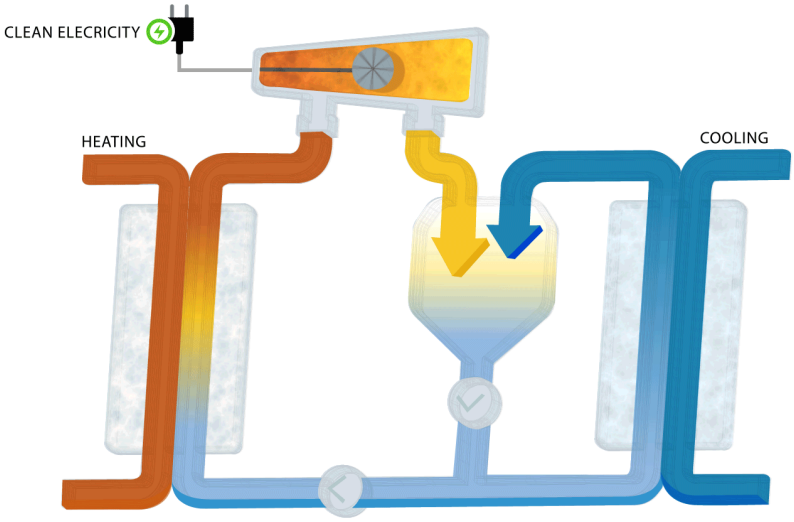

Figure 4.1: Overview of the Climeon ORC machine circuit (ClimeOn, 2017a)

4.2 Location

In the end no exact placement of the solution was achieved. Instead a recommended location, based on the discussion made in Section 3.2, was suggested. This allowed for a more straight-forward approach to evaluate and analyze the results, which is the main focus of the thesis. It also eliminates any complications regarding building permits and land ownership issues when considering the BTES system.

A recommendation was to place the ORC machine near Sävenäsverket, which is one of the larger facilities mentioned in Table 2.1. Here it can be easily handled. A nearby river, Säveån, is also available if needed as an alternate cooling source.

4.3 Data simulation

4.3.1 BTES

A BTES was designed and simulated in EED4. The base load was calculated to be 3206.75 MWh for the period May-September using the parameters described in Section 3.4.

Temperature levels calculated for a simulation period of 25 years are presented in Figure 4.2. The red curve represents the incoming fluid to the BTES system and the green curve the outgoing fluid. As can be seen from the figure, the fluid from the ORC solution would enter the BTES at approximately 35°C and would be cooled down to approximately 30°C by the BTES. During the time period when the ORC solution would not be active the BTES would be used for heating a nearby buildings

with the help of the heat pump.

Design-wise the BTES was designed using the base case parameters, however it could be adopted to other specifications by changing the flow or heat load levels.

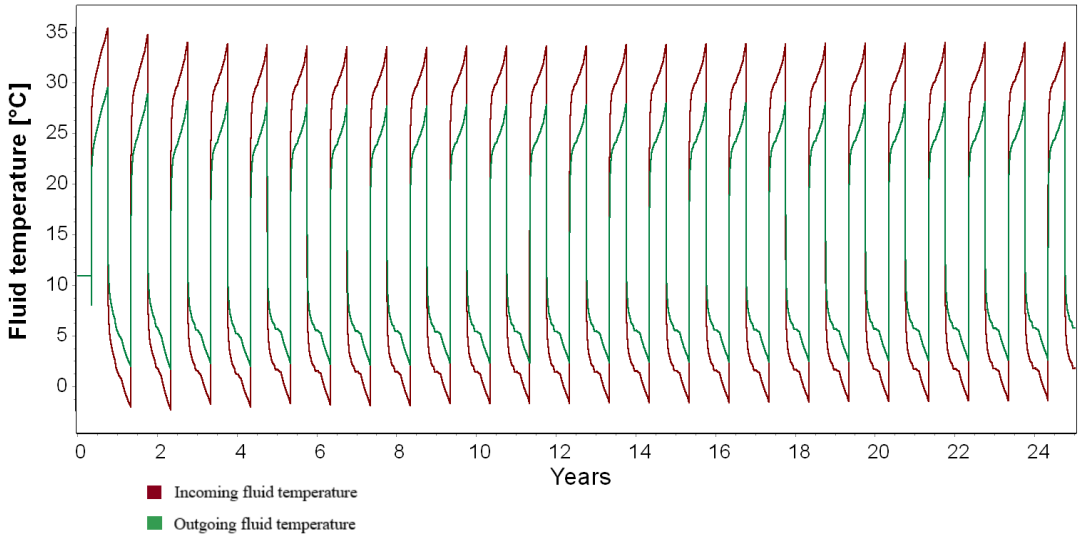

Figure 4.2: Temperature levels for a simulation time period of 25 years from EED4

4.3.2 Base case

In Table 4.1, the results for the base case simulation and calculations are presented.

Table 4.1: Results for the base case simulation and calculations

Position	Parameter	Value
Hot circuit	T_{in}	80°C
	T_{out}	74°C
	$\dot{m}_m$	34.1 kg/s
Cold circuit	T_{in}	30°C
	T_{out}	36°C
	$\dot{m}_m$	34.8 kg/s
Generator	P	56 kW
	η_{el}	6%
	E_{el}	205.6 MWh

A capacity factor of 0.42 (42%) was determined by analyzing the number of hours during the months May-September. For the base case, it was calculated that the ORC solution would operate on 37.3% of it's max capacity. The electrical efficiency was calculated to be 6% and the temperature differences on both the hot and cold side of the circuit was designed to be 6°C.

4.3.3 Sensitivity analysis

The results of the sensitivity analysis performed on the three water flow rates of 10, 35 and 50 litres per second are presented in Figures 4.3, 4.4 and 4.5, respectively. In Appendix F, the exact values for the power production are presented. The different colors in the graphs represent the cooling source temperatures and the horizontal numbers; 70, 80, 90 and 100 represents the different heat source temperatures.

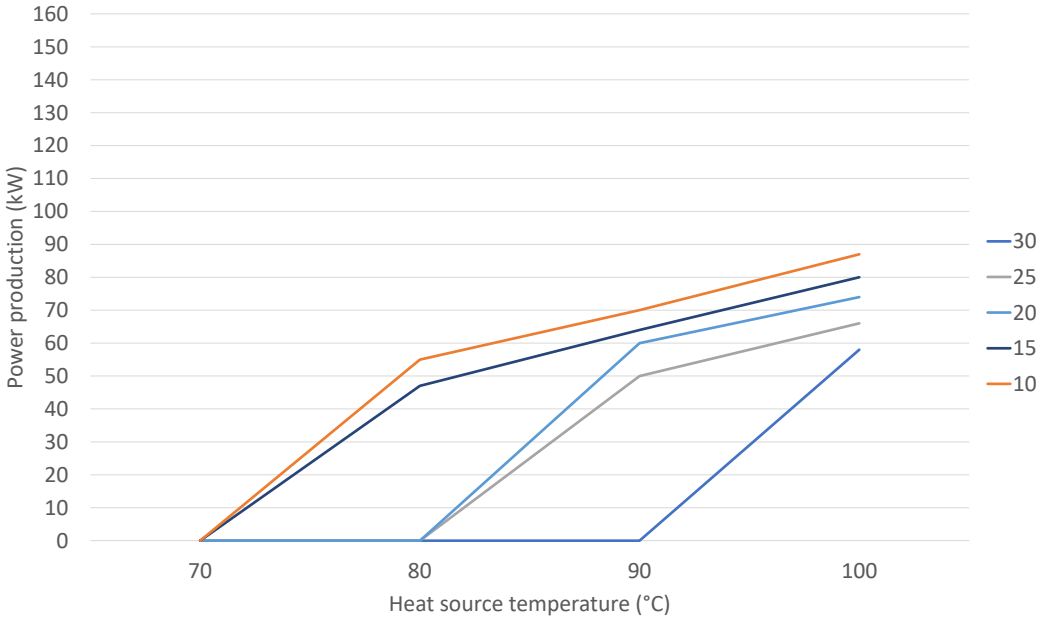

Figure 4.3: Power production for different heating and cooling source temperatures at $\dot{q} = 10$ l/s

In total, there are 11 cases where no power production was achieved by the ORC machine, and 8 cases where maximum power production was achieved. This can be seen in Appendix F. Worth noting is that a heat source temperature of 70°C and a cooling source temperature of 30°C could not generate any electrical power regardless of the water flow rate. In 6 out of the 8 cases where maximum power output was achieved, the generator limited the power to the max capacity of 150 kW for technical reasons.

For a heat source temperature of 70°C, the maximum power production that could be achieved was 72 kW at a cooling source temperature of 10°C and a water flow rate of 50 l/s. This corresponds to 48% of the maximum capacity. At a cooling source temperature of 25°C and a water flow of 35 l/s, the lowest non-zero power production was determined to be 41 kW, corresponding to 27% of the max capacity.

For a water flow rate of 10 l/s, the maximum power production was 87 kW at T_h = 100°C and T_c = 10°C, corresponding to 58% capacity. However at the same T_h, with a T_c between 10-20°C and a $\dot{q} = 35$ l/s, the power production is drastically increased to 150 kW. This shows the importance of the water flow rate.

Comparing a water flow rate of 35 l/s and 50 l/s, it could be observed that the difference in power production is not significantly large, at least when comparing to the case of $\dot{q} = 10$ l/s.

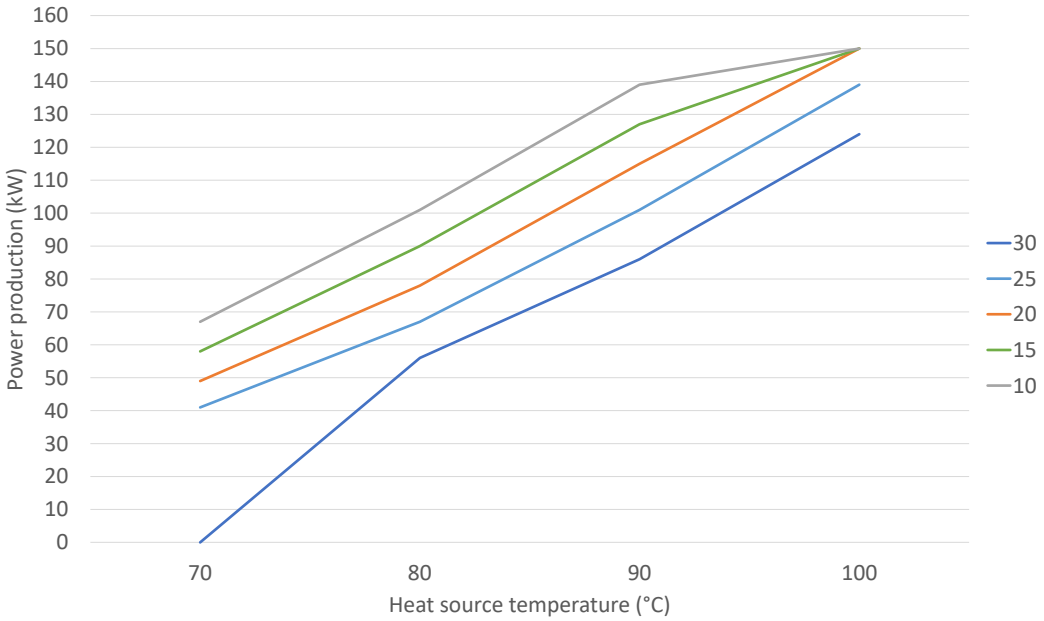

Figure 4.4: Power production for different heating and cooling source temperatures at $\dot{q} = 35$ l/s

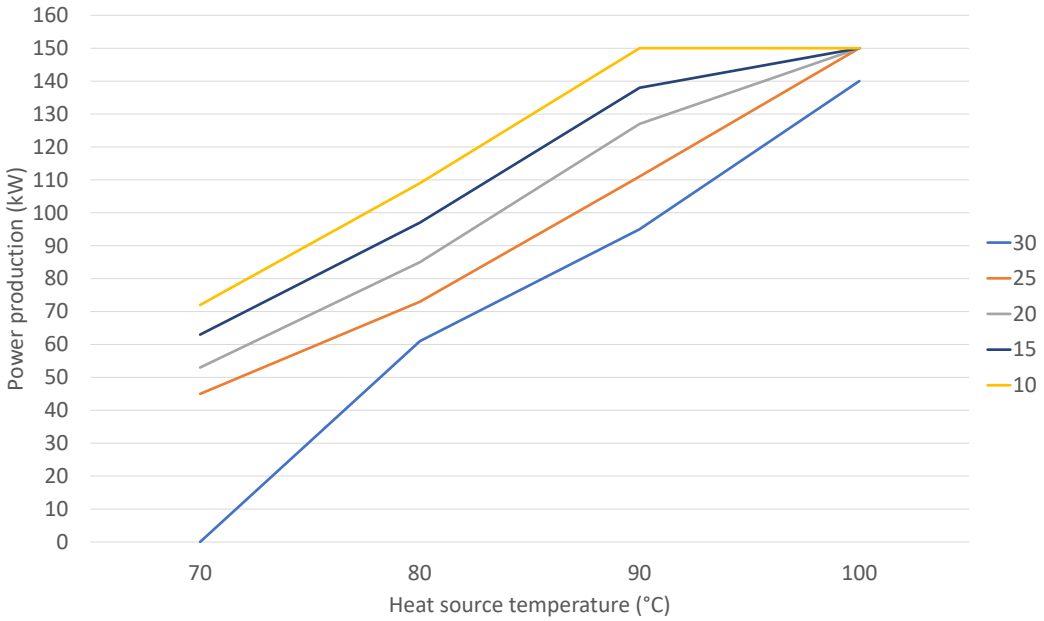

Figure 4.5: Power production for different heating and cooling source temperatures at $\dot{q} = 50$ l/s

4.3.4 Additional cases

Case 1

The results from Case 1 at $T_h = 80°C$, $T_c = 10°C$ and $\dot{q} = 35$ l/s are presented in Table 4.2.

Table 4.2: Results from Case 1 simulation

Position	Parameter	Value
Hot circuit	T_{in}	80°C
	T_{out}	73°C
	$\dot{m}_m$	34.1 kg/s
Cold circuit	T_{in}	10°C
	T_{out}	16°C
	$\dot{m}_m$	35.0 kg/s
Generator	P	101 kW
	η_{el}	10%
	E_{el}	370.9 MWh

With this configuration the ORC machine could produce 67.3% of the maximum power output with an electrical efficiency of 10%. A temperature difference of 7°C on the hot side and a difference of 6°C on the cold side were achieved respectively.

Case 2

Table 4.3 shows the configuration of Case 2 using $T_h = 90°C$, $T_c = 30°C$ and $\dot{q} = 35$ l/s.

Table 4.3: Results from Case 2 simulation

Position	Parameter	Value
Hot circuit	T_{in}	90°C
	T_{out}	82°C
	$\dot{m}_m$	33.9 kg/s
Cold circuit	T_{in}	30°C
	T_{out}	37°C
	$\dot{m}_m$	34.8 kg/s
Generator	P	86 kW
	η_{el}	8%
	E_{el}	315.8 MWh

This setup could provide power production at 57.3% capacity and an electrical efficiency of 8%. The temperature difference for the hot side was 8°C and for the cold side 7°C.

Case 3

In Table 4.4 the results from the configuration of Case 3 is shown, having T_h = 90°C, T_c = 10°C and $\dot{q}$ = 35 l/s.

Table 4.4: Results from Case 3 simulation

Position	Parameter	Value
Hot circuit	T_{in}	90°C
	T_{out}	81°C
	$\dot{m}_m$	33.9 kg/s
Cold circuit	T_{in}	10°C
	T_{out}	17°C
	$\dot{m}_m$	35.0 kg/s
Generator	P	139 kW
	η_{el}	11%
	E_{el}	510.4 MWh

During this operation 92.7% of the maximum capacity was achieved. An electrical efficiency of 11% was recorded and the temperature difference on the hot and cold side were 9°C and 7°C, respectively.

Case 4

Case 4 was simulated utilizing T_h = 90°C, T_c = 10°C and $\dot{q}$ = 50 l/s. Shown in Table 4.5.

Table 4.5: Results from Case 4 simulation

Position	Parameter	Value
Hot circuit	T_{in}	90°C
	T_{out}	84°C
	$\dot{m}_m$	48.3 kg/s
Cold circuit	T_{in}	10°C
	T_{out}	15°C
	$\dot{m}_m$	50.0 kg/s
Generator	P	150 kW
	η_{el}	12%
	E_{el}	550.8 MWh

The maximum power production was achieved for this case with a maximum electrical efficiency of 12%. Temperature differences for the hot and cold sides were 6°C and 5°C, respectively.

Case 5

Setting T_h = 90°C, T_c = 10°C and $\dot{q}$ = 50 l/s and assuming a full year of production, provides the results shown in Table 4.6. When calculating the electrical energy E_{el}

a capacity factor of 0.98 was used to account for yearly maintenance and downtime (ClimeOn, 2017b).

Table 4.6: Results from Case 5 simulation

Position	Parameter	Value
Hot circuit	T_{in}	90°C
	T_{out}	84°C
	$\dot{m}_m$	48.3 kg/s
Cold circuit	T_{in}	10°C
	T_{out}	15°C
	$\dot{m}_m$	50.0 kg/s
Generator	P	150 kW
	η_{el}	12%
	E_{el}	1287.7 MWh

4.4 Life cost analysis

Costs related to the investment of the ORC machine by Climeon are presented in Table 4.7. The Climeon Live is a software used for surveillance when operating the machine and was recommended by the company to be used. Both the service and support cost and the Climeon Live cost were summarized together as the annual cost Z in Equation 3.8. The investment cost I was inserted in Equation 3.6. Pump running costs were negligible, as parts of the power production goes directly to the machine itself, covering the electricity cost for pump work.

Table 4.7: Costs related to the Climeon module (ClimeOn, 2017b)

Type of cost	Value
Investment cost I	3.4 MSEK
Service & support cost	100 000 SEK/year
ClimeOn Live	50 000 SEK/year

The net present values were calculated for all sensitivity analysis cases and for different configurations provided. They are presented in Table 4.8 as well as depicted with the yearly values for different electricity prices in Figures 4.6, 4.7 and 4.8. As mentioned in Section 3.5.4, the life expectancy of the machine was set to 30 years and the real interest rate was set to be 9%. The results show that only Case 5 provided a positive NPV, which would indicate that the investment would only be profitable in this particular case. It is worth noting that the only case showing a positive value is the case where an all-year production was considered.

The payback periods for the two cases where the NPV is positive were approximately 28 years for Case 5 considering a mean electricity price and around 10 years for Case 5 considering a high electricity price, see Figures 4.7 and 4.8. The rest of the cases

did not achieve a payback period within the lifespan of the ORC solution. Looking at a low electricity price, the net present value is decreasing over the years, indicating that the yearly revenues would not be enough to cover the costs.

Table 4.8: Total net present values for the base case & Cases 1-5 at three different electricity prices

Case	Electricity price (SEK/MWh)	NPV (SEK)
BC	$Y_{el,low} = 85.0$	-5 438 258
BC	$Y_{el,m} = 282.5$	-4 805 114
BC	$Y_{el,high} = 448.4$	-4 273 274
C1	$Y_{el,low} = 85.0$	-5 202 325
C1	$Y_{el,m} = 282.5$	-4 060 406
C1	$Y_{el,high} = 448.4$	-3 101 194
C2	$Y_{el,low} = 85.0$	-5 280 970
C2	$Y_{el,m} = 282.5$	-4 308 642
C2	$Y_{el,high} = 448.4$	-3 491 887
C3	$Y_{el,low} = 85.0$	-5 003 094
C3	$Y_{el,m} = 282.5$	-3 431 541
C3	$Y_{el,high} = 448.4$	-2 111 437
C4	$Y_{el,low} = 85.0$	-4 945 421
C4	$Y_{el,m} = 282.5$	-3 249 501
C4	$Y_{el,high} = 448.4$	-1 824 929
C5	$Y_{el,low} = 85.0$	-3 835 536
C5	$Y_{el,m} = 282.5$	129 370
C5	$Y_{el,high} = 448.4$	3 459 890

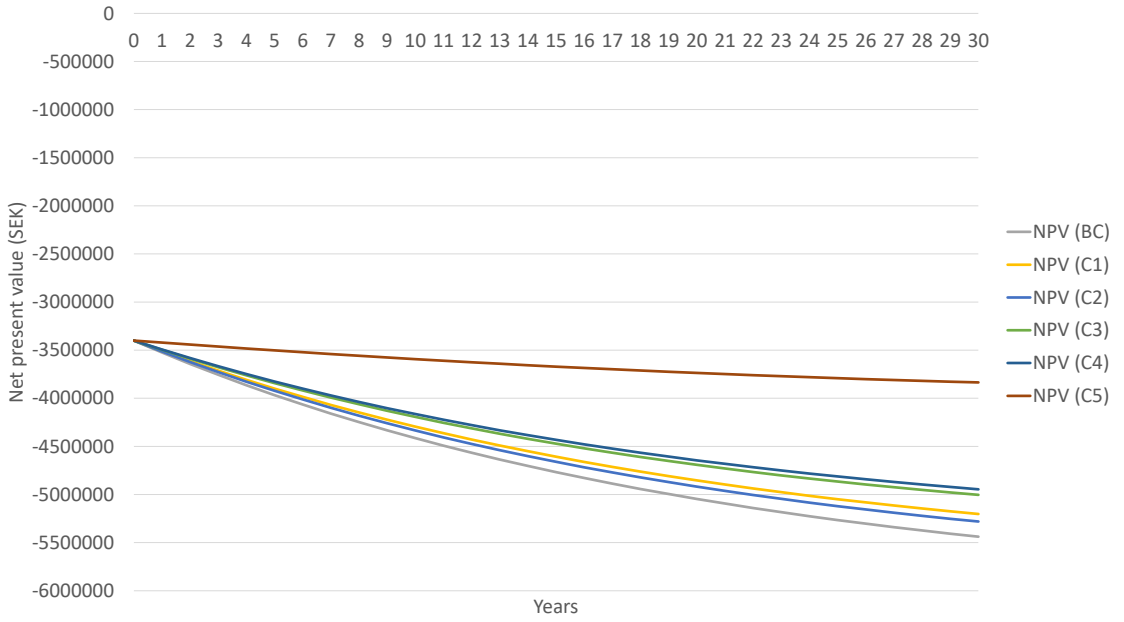

Figure 4.6: The net present value over a time period of 30 years considering the low electricity price of 85 SEK/MWh

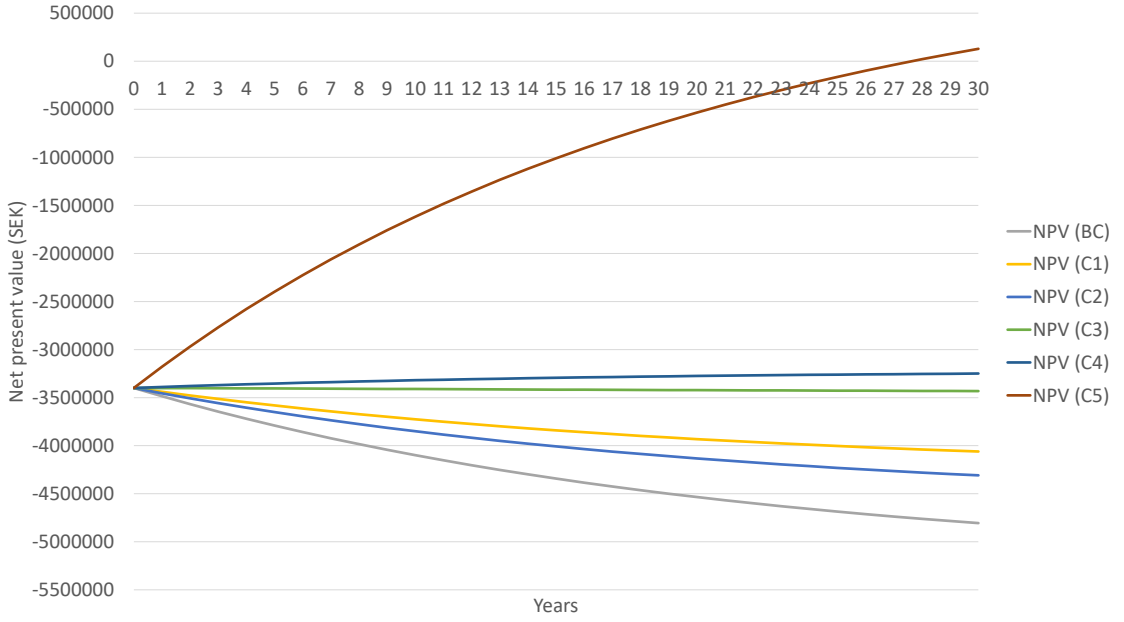

Figure 4.7: The net present value over a time period of 30 years considering the mean electricity price of 282.5 SEK/MWh

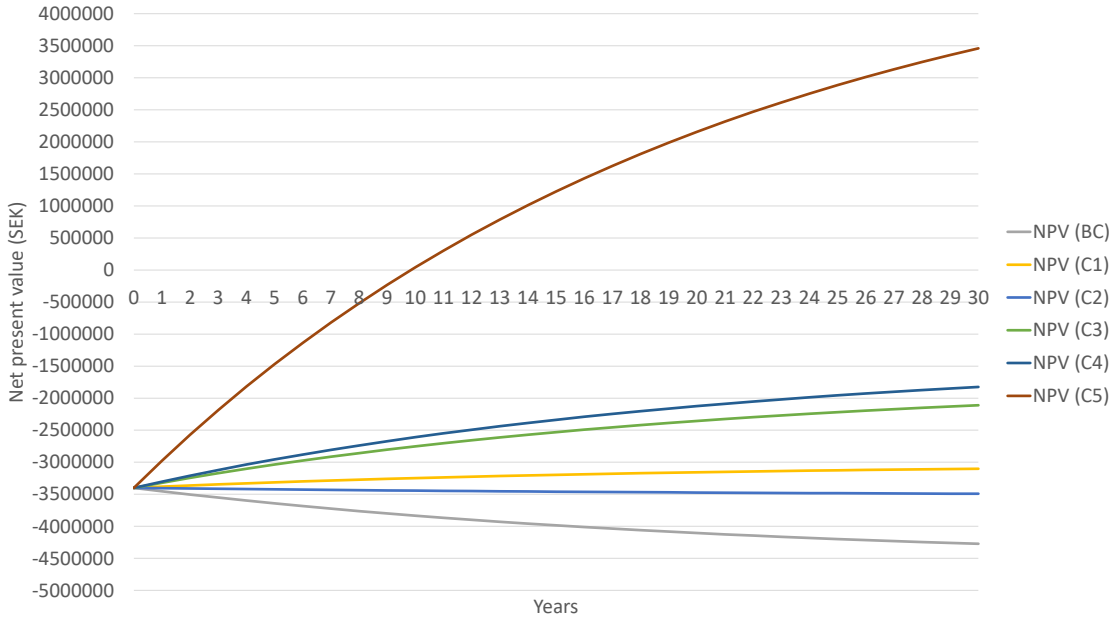

Figure 4.8: The net present value over a time period of 30 years considering the high electricity price of 448.4 SEK/MWh

5
Discussion & conclusions

One kilogram of oil produce 41 800 kJ of total energy, whilst one kilogram of high-quality steam yields 3000 kJ. In comparison to an ORC setup using hot water at 80°C inlet temperature and 30°C outlet temperature on the heating side of the circuit, gives only 209 kJ (Barbier, 2002), which is equivalent to 0.5% of the energy provided from the oil. A comparison like this proves that low-temperature energy sources are far from efficient when only considering the energy production. When comparing the results of the case studies in Section 2.3.3 with the results from this report, the numbers are fairly similar with a slight advantage of the Climeon module in terms of electrical efficiency. This partially proves that the chosen solution is in fact a state-of-the-art solution, which presents results that can be difficult to improve.

Increase of mean seasonal outdoor air temperatures will affect the future of district heating systems, which will in turn affect solutions similar to the one presented in the thesis. In such a scenario, the overall flow rates and cooling source temperatures of an ORC solution will become highly important due to the lowered district heating supply temperatures. Furthermore, in Sweden the district heating systems have come to a stagnation point in terms of heat supply and demand since the mid 1990s. This trend could make it interesting to implement such a solution in the existing DH systems to make use of the energy potential that still exists (Magnusson, 2012).

Weather-based solutions for power production have been proven to be unpredictable in terms of production, and an ORC solution powered by a district heating system is no different. As it is affected by the outdoor air temperature, it is fairly difficult to pin-point the exact power production. Nevertheless, it is still possible to make estimations using statistical data or via mathematical models (Bremen, 2010). A more predictable way would be to connect a deep geothermal well to the heating side of the ORC circuit, as proven by a few of the case studies mentioned in Section 2.3.3. This could potentially stabilize the power production.

The solution should at all times be operating at the maximum flow rate if possible. As seen from the sensitivity analysis in Section 4.3.3, a water flow rate of 50 l/s was needed to produce maximum power production at a heat source temperature of 90°C and a cooling source temperature of 10°C. This was confirmed by Cases 4 and 5 in the results section. Overall a higher flow rate improves the power production for all temperature configurations and does not prove to be disadvantageous result-wise. A large system like the district heating system should be able to produce this kind

of flow rate, but if the overall flow rate of the system is not adequate enough, pumps might be needed to increase the rate. This could affect the profitability due to the potential investment of a pump as well as running costs.

Furthermore, a solution like this could benefit more by having a larger capacity factor. As proven by the results from the base case simulation in Section 4.3.2 and the results from the economical calculations in Section 3.5.4, a capacity factor of 0.42 was hardly beneficial economically, especially not when considering such low power production. It is at the same time difficult to predict the amount of excess heat produced during the winter when the demand for district heating is larger. Therefore the electrical energy production can be very difficult to evaluate before-hand. In order to reach the economical break-even point for a high electricity price considering maximum power production the capacity factor is required to be 0.612, which corresponds to approximately 5361 hours of operation time, or 804.2 MWh. This is equivalent to slightly over seven months of operation opposed to the five months used in the first five cases.

The thesis did not take into account the costs related to the drilling and installation of a BTES system, nor the heat source costs for the ORC solution and the potential revenues that could be gained from selling stored heat in the BTES. These parameters could impact the profitability greatly. The added annual cost Z of the ORC solution also played a huge roll economically. If this cost could be reduced or removed entirely, a positive annual net profit is most likely to occur for some of the cases. From the results shown only Case 5 resulted in a positive payback, i.e with the mean and high electricity prices considered. However, the solution was considered to be operating the whole year round, which proves that the solution is in fact required to be used to this extent in order to make the investment profitable.

Looking at the electricity price, a mean electricity price proved in Case 5 to be a minimal requirement for profitability. The payback period for the mean electricity price was 28 years, which is only two years less than the lifetime of the solution. A result like this shows that the solution requires an above average electricity price at all times to be profitable. This can not always be guaranteed considering the fluctuations of the electricity prices.

To further improve the cash flow of the investment, the district heating system can be improved by adding more renewable energy sources that produces heat. In this way the amount of electricity certificates can be increased, hence increasing the revenues. Something to consider as well is that by increasing the number of renewables used, the electricity prices in general might be affected which also has to be accounted for.

The interest rate also plays a huge roll financially as high interest rates decrease the net present value. An investment like this could benefit greatly by a lower interest rate. If the nominal interest rate is decreased to 5% and the real interest rate to 3%, the payback period for Case 5 with a mean electricity price is instead 15 years,

down from 28 years. For the high electricity price, the difference is less remarkable, with a decrease from 10 to 8 years. This shows the importance of the interest rate, especially when the electricity price is around the mean value. However, in this case, the rate is decided entirely on how the investors view the investment and this can be a difficult parameter to affect.

In conclusion the options available for power production using low-temperature heat as a energy source are extremely limited and an ORC solution is most likely to be the most effective one. It is a unique solution in it self and therefore fairly difficult to compare to other alternatives. Only the future will reveal newer, more innovative and competitive technologies that can be weighed against the proposed solution.

In summary, a solution was successfully found and virtually placed inside the district heating system of Gothenburg. Design and simulation of a BTES was also carried out, and in the end all the various simulation cases were evaluated. It was proven that Case 4 produced the most amount of power with the least amount of work input during months May-September. The total amount of electrical energy produced during this time was determined to be 550.8 MWh. When considering an all year production, the electrical energy was instead 1287.7 MWh. The results from the life cost analysis showed that the solution was highly dependent on the electricity prices to be profitable. In addition, the ORC solution also needed to operate all year round to yield a positive NPV.

Bibliography

Abhat, A. (1981). Short term thermal energy storage. *Energy and Buildings*, 3(1):49 – 76.

Ahlbom, E. (2017). Removal of non-condensable gases from a closed loop process. US Patent App. 15/301,350.

Aneke, M., Agnew, B., and Underwood, C. (2011). Performance analysis of the chena binary geothermal power plant. *Applied Thermal Engineering*, 31(10):1825 – 1832.

Barbier, E. (2002). Geothermal energy technology and current status: an overview. *Renewable and Sustainable Energy Reviews*, 6(1):3 – 65.

Borsukiewicz-Gozdur, A. (2013). Experimental investigation of r227ea applied as working fluid in the orc power plant with hermetic turbogenerator. *Applied Thermal Engineering*, 56(1):126 – 133.

Bremen, L. V. (2010). Large-scale variability of weather dependent renewable energy sources. In Troccoli, A., editor, *Management of Weather and Climate Risk in the Energy Industry*, pages 189–206, Dordrecht. Springer Netherlands.

Calnetix Technologies (2014). Hydrocurrent™ Organic Rankine Cycle (ORC) Module 125EJW. `https://www.calnetix.com/sites/default/files/Calnetix_Hydrocurrent_ORC_Brochure_web.pdf`. Retrieved 2017-11-02.

Claesson, J. and Javed, S. (2018). Explicit multipole formulas for calculating thermal resistance of single u-tube ground heat exchangers. *Energies*, 11(1).

ClimeOn (2017a). How it works. `https://www.climeon.com/how-it-works/`. Retrieved 2017-12-11.

ClimeOn (2017b). INBJUDAN TILL FÖRVÄRV AV B-AKTIER I CLIMEON AB (PUBL). `https://climeon.com/uploads/2017/09/Climeon-AB-Prospekt-September-2017.pdf`. Retrieved 2017-12-11.

ClimeOn (2017c). TECHNICAL PRODUCT SHEET. `https://climeon.com/uploads/2017/04/Climeon-Tech-Product-Sheet.pdf`. Retrieved 2017-11-13.

DuPont (2009). *DuPont™ FM-200® Fire Extinguishing Agent.*

E-rational (2017). Data Sheets. `http://www.e-rational.net/downloads/brochures`. Retrieved 2017-11-07.

ElectraTherm (2017). What is a Power+ Generator™? https://electratherm.com/orc-knowledge-center-2/what-is-a-power-plus-generator/. Retrieved 2017-11-07.

Energimyndigheten (2018a). The Electricity Certificate System. http://www.energimyndigheten.se/en/sustainability/the-electricity-certificate-system/. Retrieved 2018-01-12.

Energimyndigheten (2018b). Statistics Elcertificates - Average Price. https://cesar.energimyndigheten.se/WebPartPages/AveragePricePage.aspx. Retrieved 2018-01-28.

Erbaş, M. and Biyikoglu, A. (2013). Design of low temperature organic rankine cycle and turbine. In *4th International Conference on Power Engineering, Energy and Electrical Drives*, pages 1065–1070.

Florides, G. and Kalogirou, S. (2007). Ground heat exchangers—a review of systems, models and applications. *Renewable Energy*, 32(15):2461 – 2478.

Forsgren, H. (2017). Presentation about Göteborg Energi for ClimeOn.

Gadd, H. and Werner, S. (2014). Achieving low return temperatures from district heating substations. *Applied Energy*, 136:59 – 67.

GB Energy Europe (2017). E-RATIONAL 1000 SERIES. http://www.gborc.eu/e-rational-1000-series. Retrieved 2017-11-07.

Göteborg Energi (2012). Heat generation in the DH system of Göteborg 2012.

Göteborg Energi (2016a). Miljövärden för levererad fjärrvärme 2016, Göteborg, Partille och Ale (exkl. Bra Miljöval). https://www.goteborgenergi.se/Files/Bilder/Fjarrvarme/Milj%C3%B6v%C3%A4rden%20f%C3%B6r%20fj%C3%A4rrv%C3%A4rme%202016%20Prelimin%C3%A4ra.pdf?TS=636214469438536170. Retrieved 2018-01-12.

Göteborg Energi (2016b). Tekniska bestämmelser för fjärrvärmecentraler. https://www.goteborgenergi.se/Files/Bilder/Fjarrvarme/Tekniska%20best%c3%a4mmelser%20f%c3%b6r%20Fj%c3%a4rrv%c3%a4rmecentraler%202016-01-01.pdf?TS=635912922045765092. Retrieved 2017-10-23.

Göteborg Energi (2017a). Göteborg Energi - District heating. https://www.goteborgenergi.se/English/Products/District_heating. Retrieved 2017-09-27.

Göteborg Energi (2017b). Produktionsanläggningar för fjärrvärme. https://www.goteborgenergi.se/Om_oss/Var_verksamhet/Produktionsanlaggningar. Retrieved 2017-10-25.

Göteborg Energi (2017c). DLS - Drift Lednings System. Sent as a file named "FV-dataSpillvärmeel.xlsx". Retrieved 2017-11-04.

Göteborg Energi (2017d). Conversation with Lennart Hjalmarsson, Göteborg Energi.

Göteborg Energi (2017e). Fjärrvärmepris 2017. https://www.goteborgenergi.se/Foretag/Produkter_och_tjanster/Fjarrvarme/Priser. Retrieved 2017-10-23.

Göteborg Energi (2017f). Vårt fjärrvärmenät. https://www.goteborgenergi.se/Privat/Produkter_och_priser/Fjarrvarme/Om_fjarrvarme/Karta_over_fjarrvarmenatet. Retrieved 2017-10-20.

Hung, T., Shai, T., and Wang, S. (1997). A review of organic rankine cycles (orcs) for the recovery of low-grade waste heat. *Energy*, 22(7):661 – 667.

Hung, T., Wang, S., Kuo, C., Pei, B., and Tsai, K. (2010). A study of organic working fluids on system efficiency of an orc using low-grade energy sources. *Energy*, 35(3):1403 – 1411.

Hung, T.-C. (2001). Waste heat recovery of organic rankine cycle using dry fluids. *Energy Conversion and Management*, 42(5):539 – 553.

ICAX™ (2018). BTES - Borehole Thermal Energy Storage - saving carbon emissions by re-cycling Renewable Heat through Interseasonal Heat Stores - Seasonal Heat Storage. https://www.icax.co.uk/Borehole_Thermal_Energy_Storage.html. Retrieved 2018-03-15.

Javed, S. (2012). *Thermal Modelling and Evaluation of Borehole Heat Transfer*. PhD thesis, Chalmers University of Technology.

Javed, S. (2013). Thermal response testing: Results and experiences from a ground source heat pump test facility with multiple boreholes. Proceedings of 11th REHVA World Congress (Clima 2013).

Javed, S. and Spitler, J. (2016). 3 - calculation of borehole thermal resistance. In Rees, S. J., editor, *Advances in Ground-Source Heat Pump Systems*, pages 63 – 95. Woodhead Publishing.

Javed, S. and Spitler, J. (2017). Accuracy of borehole thermal resistance calculation methods for grouted single u-tube ground heat exchangers. *Applied Energy*, 187(C):790–806.

Kolasiński, P. (2015). The influence of the heat source temperature on the multi-vane expander output power in an organic rankine cycle (orc) system. *Energies*, 8(5):3351–3369.

Kosmadakis, G., Landelle, A., Lazova, M., Manolakos, D., Kaya, A., Huisseune, H., Karavas, C.-S., Tauveron, N., Revellin, R., Haberschill, P., Paepe, M. D., and Papadakis, G. (2016). Experimental testing of a low-temperature organic rankine cycle (orc) engine coupled with concentrating pv/thermal collectors: Laboratory and field tests. *Energy*, 117(Part 1):222 – 236.

Lund, H., Werner, S., Wiltshire, R., Svendsen, S., Thorsen, J. E., Hvelplund, F., and Mathiesen, B. V. (2014). 4th generation district heating (4gdh): Integrating smart thermal grids into future sustainable energy systems. *Energy*, 68(Supplement C):1 – 11.

Magnusson, D. (2012). Swedish district heating—a system in stagnation: Current and future trends in the district heating sector. *Energy Policy*, 48:449 – 459. Special Section: Frontiers of Sustainability.

Minea, V. (2014). Power generation with orc machines using low-grade waste heat or renewable energy. *Applied Thermal Engineering*, 69(1):143 – 154.

Mitsubishi Heavy Industries Marine Machinery & Engine Co., Ltd. (2015). Hydrocurrent™ Organic Rankine Cycle Module 125EJW - Compact and High-performance Waste Heat Recovery System Utilizing Low Temperature Heat Source -. `https://www.mhi.com/company/technology/review/pdf/e524/e524053.pdf`. Retrieved 2017-11-07.

Moskvicheva, V. and Popov, A. (1970). Geothermal power plant on the paratunka river. *Geothermics*, 2(Part 2):1567 – 1571. Proceedings of the United Nations symposium on the development and utilization of geothermal resources.

Myriad (2017). ORGANIC RANKINE CYCLE. `http://www.myriadceg.com/orc-electricity-waste-heat`. Retrieved 2017-11-08.

Nielsen, K. (2003). Thermal energy storage a state-of-the-art. Technical report, Smart Energy-Efficient Buildings, NTNU.

Nord Pool (2018). Day-ahead prices. `https://www.nordpoolgroup.com/Market-data1`. Retrieved 2018-01-10.

Nordell, B. (1994). *Borehole heat store design optimization*. PhD thesis, Luleå University of Technology, Architecture and Water. Approved; 1994; 20070209 (ysko).

Orcan Energy AG (2017). Datasheet: ePACK M 040.100 HD. `http://www.orcan-energy.com/sites/default/files/OrcanEnergy_Marine_DS_HD_web_EN.pdf`. Retrieved 2017-11-07.

Pahud, D. and Fromentin, A. (1999). Pilesim: a simulation tool for pile and borehole heat exchanger systems. Bulletin d'Hydrogéologie 17, Centre d'Hydrogéologie, University of Neuchatel, Neuchatel, Switzerland.

Pahud, D. and Matthey, B. (2001). Comparison of the thermal performance of double u-pipe borehole heat exchangers measured in situ. *Energy and Buildings*, 33(5):503 – 507. Special Issue: Proceedings of the International Conference on.

Persson, T., Stavset, O., Ramstad, R. K., Alonso, M. J., and Lorenz, K. (2016). Software for modelling and simulation of ground source heating and cooling systems. Technical Report TR A7570, Dalarna University, Energy Technology. Research Council of Norway.

Pikra, G., Rohmah, N., Pramana, R. I., and Purwanto, A. J. (2015). The electricity power potency estimation from hot spring in indonesia with temperature 70-80°c using organic rankine cycle. *Energy Procedia*, 68(Supplement C):12 – 21. 2nd International Conference on Sustainable Energy Engineering and Application (ICSEEA) 2014 Sustainable Energy for Green Mobility.

Popiel, C., Wojtkowiak, J., and Biernacka, B. (2001). Measurements of temperature distribution in ground. *Experimental Thermal and Fluid Science*, 25(5):301 – 309.

Quoilin, S., Declaye, S., Tchanche, B. F., and Lemort, V. (2011). Thermo-economic optimization of waste heat recovery organic rankine cycles. *Applied Thermal Engineering*, 31(14):2885 – 2893.

Reuss, M., Beck, M., and Müller, J. (1997). Design of a seasonal thermal energy storage in the ground. *Solar Energy*, 59(4):247 – 257. Selected Proceeding of ISES 1995: Solar World Congress. Part IV.

Rybach, L. and Hopkirk, R. J. (1995). Shallow and deep borehole heat exchangers - achievements and prospects. In *SECTION 10 - Direct Heat Uses*, World Geothermal Congress, pages 2133 – 2138. International Geothermal Association.

Sang, L. K. (2010). Simulation on the cyclic operation of an open borehole thermal energy storage system under regional groundwater flow. *Geosciences Journal*, 14(2):217–224.

Sanner, B., Karytsas, C., Mendrinos, D., and Rybach, L. (2003). Current status of ground source heat pumps and underground thermal energy storage in europe. *Geothermics*, 32(4):579 – 588. Selected Papers from the European Geothermal Conference 2003.

Schmidt, T. and Mangold, D. (2006). New steps in seasonal thermal energy storage in germany. In *Ecostock 2016*, 10th International Conference on Thermal Energy Storage.

SGU, Geological Survey of Sweden (2017). Bedrock map. `http://apps.sgu.se/kartgenerator/maporder_en.html`. Retrieved 2017-12-12.

Sibbitt, B., McClenahan, D., Djebbar, R., Thornton, J., Wong, B., Carriere, J., and Kokko, J. (2012). The performance of a high solar fraction seasonal storage district heating system – five years of operation. *Energy Procedia*, 30(Supplement C):856 – 865. 1st International Conference on Solar Heating and Cooling for Buildings and Industry (SHC 2012).

Siiskonen, M. (2015). Seasonal low temperature borehole thermal energy storage. Master's thesis, Chalmers University of Technology.

SMHI (2017). Meteorologiska observationer. `http://opendata-download-metobs.smhi.se/explore/`. Retrieved 2017-11-21.

Socaciu, L. (2011). Seasonal sensible thermal energy storage solutions. *Leonardo Electronic Journal of Practices and Technologies*, 10:49–68.

Spitler, G. J. D., Marshall, C. L., Manickam, A., Dharapuram, M., Delahoussaye, R., Yeung, K.-W. D., Young, R., Bhargava, M., Mokashi, S., Yavuzturk, C., Haider, M., Xu, X., Cullin, J., Dickinson, B., Lee, E., and Grundmann, R. (2016a). *GLHEPro 5.0 For Windows - Users' Guide*. International Ground Source Heat Pump Association, School of Mechanical and Aerospace Engineering Oklahoma State University.

Spitler, J. D., Javed, S., and Ramstad, R. K. (2016b). Natural convection in groundwater-filled boreholes used as ground heat exchangers. *Applied Energy*, 164:352 – 365.

Tchanche, B. F., Lambrinos, G., Frangoudakis, A., and Papadakis, G. (2011). Low-grade heat conversion into power using organic rankine cycles – a review of various applications. *Renewable and Sustainable Energy Reviews*, 15(8):3963 – 3979.

Vieira, A., Maranha, J., Christodoulides, P., Alberdi-Pagola, M., Loveridge, F., Nguyen, F., Florides, G., Radioti, G., Cecinato, F., Prodan, I., Ramalho, E., Georgiev, A., Rosin-Paumier, S., Lenart, S., Erbs Poulsen, S., Popov, R., Lenart, S., Erbs Poulsen, S., Radioti, G., Javed, S., Van Lysebetten, G., and Salciarini, D. (2017). Characterisation of ground thermal and thermo-mechanical behaviour for shallow geothermal energy applications. *Energies*, 10(12).

Viking Heat Engines (2017). CraftEngine: An ORC heat engine designed for any challenge. `http://www.vikingheatengines.com/products`. Retrieved 2017-11-08.

Werner, S. (1989). *Fjärrvärmens utbredning och utveckling*. Värmeföreningen, Stockholm.

Werner, S. (2017). District heating and cooling in Sweden. *Energy*, 126:419–429. https://doi.org/10.1016/j.energy.2017.03.052.

Weron, R. (2014). Electricity price forecasting: A review of the state-of-the-art with a look into the future. *International Journal of Forecasting*, 30(4):1030 – 1081.

Zeng, H., Diao, N., and Fang, Z. (2003). Heat transfer analysis of boreholes in vertical ground heat exchangers. *International Journal of Heat and Mass Transfer*, 46(23):4467 – 4481.

Zhai, X., Qu, M., Yu, X., Yang, Y., and Wang, R. (2011). A review for the applications and integrated approaches of ground-coupled heat pump systems. *Renewable and Sustainable Energy Reviews*, 15(6):3133 – 3140.

Zhang, X., Wu, L., Wang, X., and Ju, G. (2016). Comparative study of waste heat steam src, orc and s-orc power generation systems in medium-low temperature. *Applied Thermal Engineering*, 106(Supplement C):1427 – 1439.

Appendix A

District heating system of Gothenburg

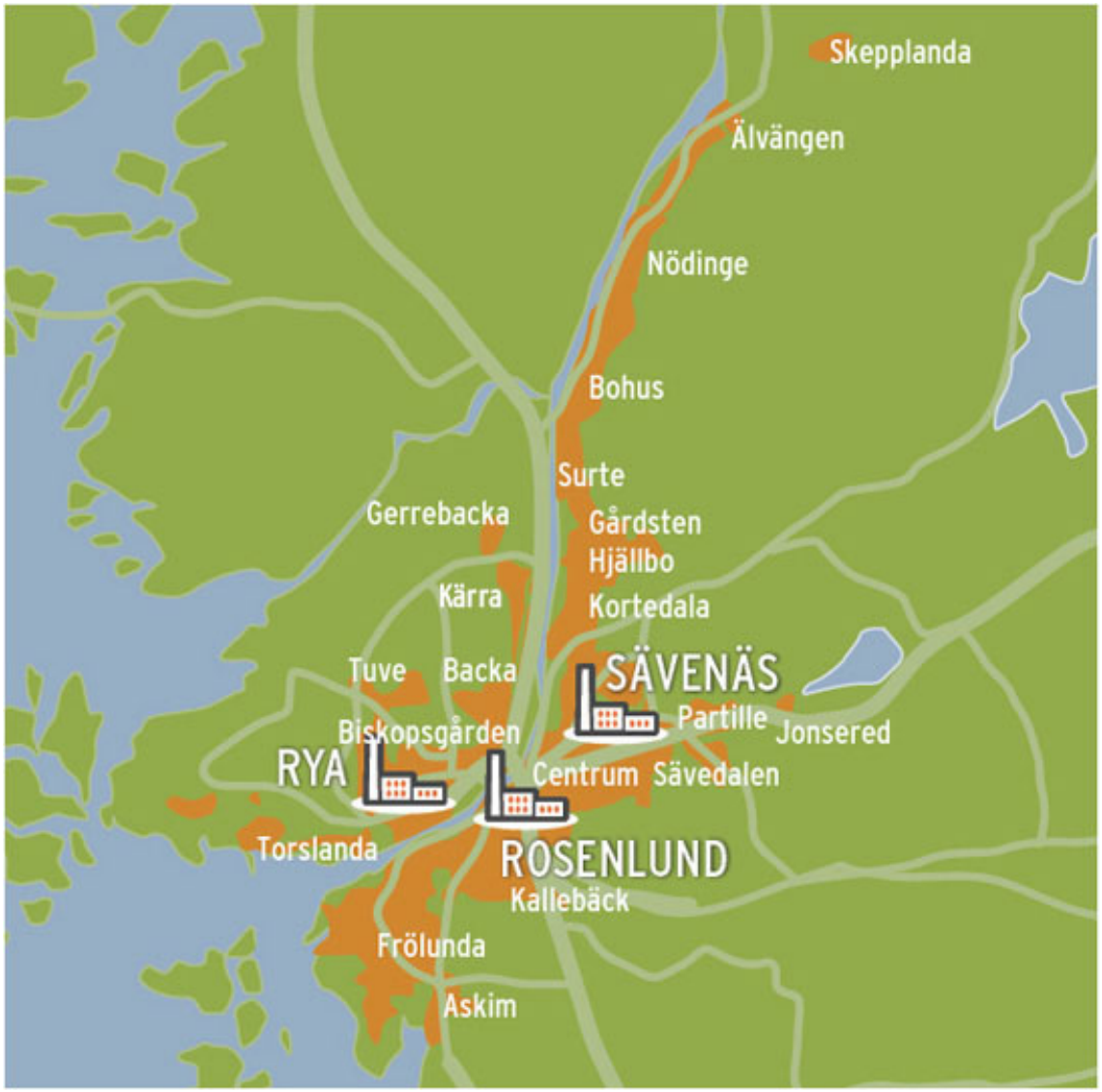

Figure A.1: Overview of areas (shown in orange) covered by the district heating system (Göteborg Energi, 2017f)

Appendix B

Prices of electricity certificates

Average price per month

28.01.2018 17:38:20

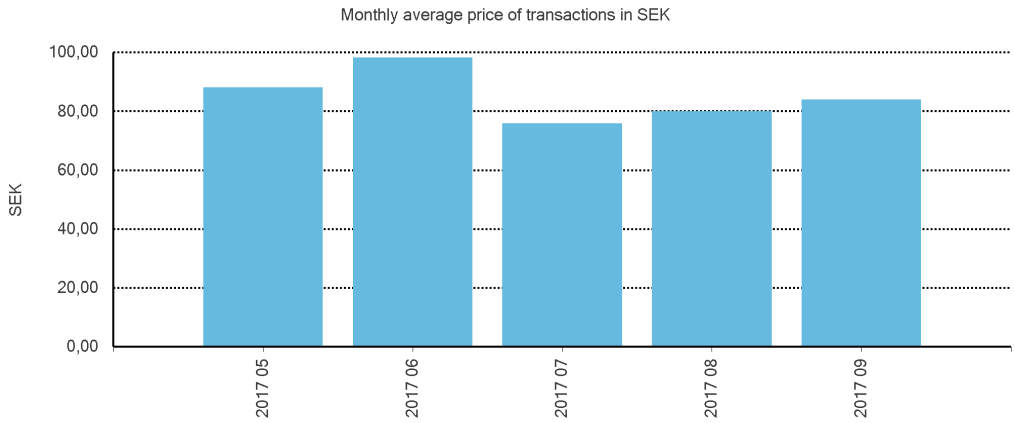

Average price for the chosen period*		
2017-05 To 2017-09	86,09	SEK

Month	Average price per month	
2017 09	84,07	SEK
2017 08	80,00	SEK
2017 07	75,96	SEK
2017 06	98,35	SEK
2017 05	88,19	SEK

Currency details	
Currency	SEK
Exchange rate of	2018-01-26
1 EUR	9,5655 NOK
1 EUR	9,8005 SEK

Figure B.1: Recent price development of electricity certificates from May-September in 2017 (Energimyndigheten, 2018b)

Average price per month

04.02.2018 16:19:05

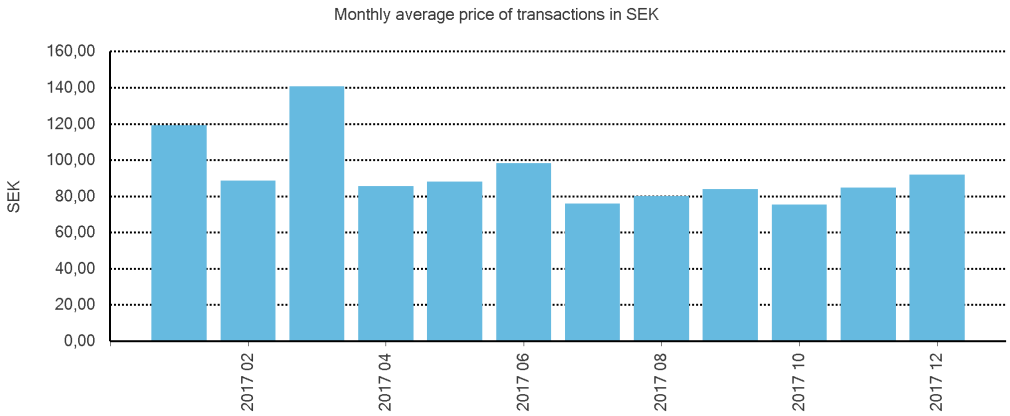

Average price for the chosen period*		
2017-01 To 2017-12	123,66	SEK

Month	Average price per month	
2017 12	91,93	SEK
2017 11	84,98	SEK
2017 10	75,40	SEK
2017 09	84,10	SEK
2017 08	80,05	SEK
2017 07	76,00	SEK
2017 06	98,39	SEK
2017 05	88,22	SEK
2017 04	85,74	SEK
2017 03	140,92	SEK
2017 02	88,84	SEK
2017 01	119,20	SEK

Currency details	
Currency	SEK
Exchange rate of	2018-02-02
1 EUR	9,5663 NOK
1 EUR	9,8223 SEK

Figure B.2: Recent price development of electricity certificates for the year 2017 (Energimyndigheten, 2018b)

Appendix C

Bedrock types in Gothenburg

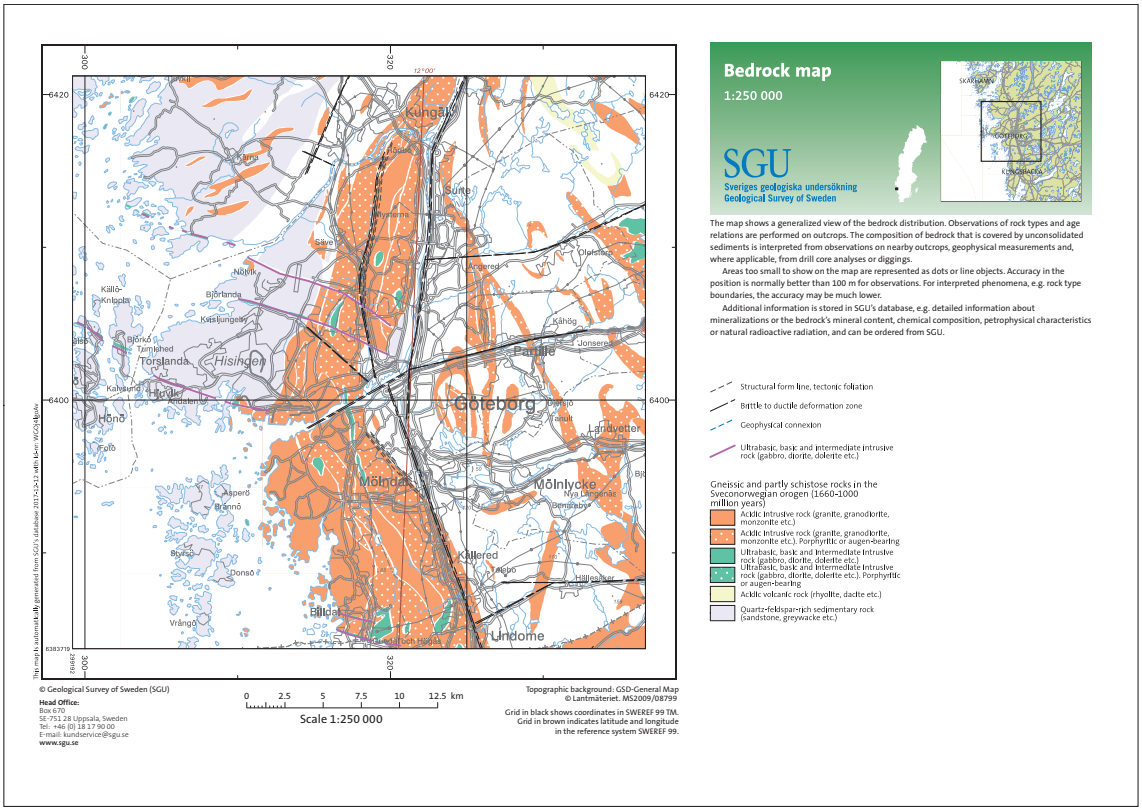

Figure C.1: Topographical map of the bedrock types in Gothenburg (SGU, Geological Survey of Sweden, 2017)

Appendix D

U-tube layout and borehole formation

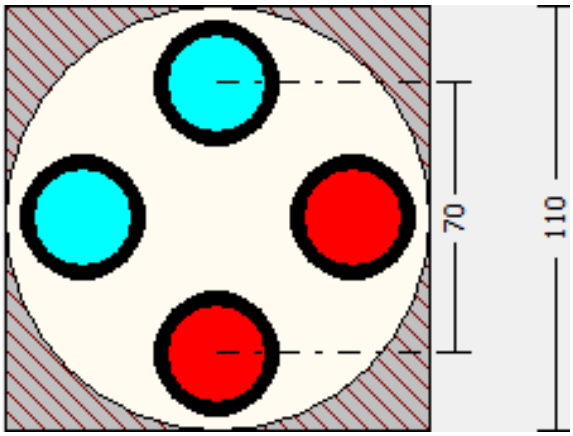

Figure D.1: Double u-pipe dimensions of the BTES system

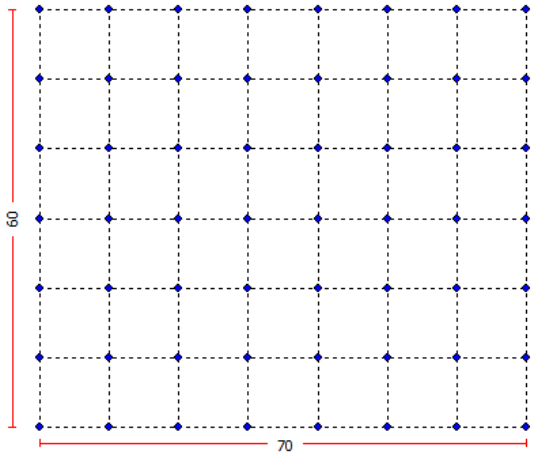

Figure D.2: Borehole formation - 7x8

Appendix E

Climeon technical product sheet

SPECIFICATIONS CLIMEON HEATPOWER SYSTEM		
MODULE	**ONE MODULE 150 kW**	**POWERBLOCK (7 modules) 1 MW**
Height *mm*	2270	2270
Depth *mm*	2105	2105
Width *mm*	2085	14700
Weight *kg (total)*	9000	63000
ELECTRICAL CABINET		
Height *mm*	2100	2100
Depth *mm*	600	600
Width *mm*	2200	13600
Weight *kg*	1200	6100
HEATING CIRCUIT		
Module flange connections *ISO*	DN125/PN10	DN125/PN10
Flow rate *l/s*	10-50	70-350
Inlet temperature *max* °C	120	120
COOLING CIRCUIT		
Module flange connections *ISO*	DN125/PN6	DN125/PN6
Flow rate *l/s*	10-50	70-350
Min cooling inlet temp. °C	0	0
Max cooling inlet temp. °C	35	35
ELECTRICAL SPECIFICATION		
Max net output power *kW*	150	1050
Voltage selectable *V*	400/690	400/690
Frequency selectable *Hz*	50/60	50/60

Figure E.1: Parameters for the Climeon Module and Powerblock (ClimeOn, 2017c)

Appendix F

Sensitivity analysis of power production

Table F.1: Power production (kW) for different temperatures at a water flow rate of 10 l/s

$\dot{q}$ [l/s]; 10		T_h [°C]			
		70	80	90	100
T_c [°C]	30	-	-	-	58
	25	-	-	50	66
	20	-	-	60	74
	15	-	47	64	80
	10	-	55	70	87

Table F.2: Power production (kW) for different temperatures at a water flow rate of 35 l/s

$\dot{q}$ [l/s]; 35		T_h [°C]			
		70	80	90	100
T_c [°C]	30	-	56	86	124
	25	41	67	101	139
	20	49	78	115	150
	15	58	90	127	150
	10	67	101	139	150

Table F.3: Power production (kW) for different temperatures at a water flow rate of 50 l/s

$\dot{q}$ [l/s]; 50		T_h [°C]			
		70	80	90	100
T_c [°C]	30	-	61	95	140
	25	45	73	111	150
	20	53	85	127	150
	15	63	97	138	150
	10	72	109	150	150